Old Dominion University

# ODU Digital Commons

2021

# Photodynamic Therapy of Inorganic Complexes for the Treatment of Cancer

Chloe B. Smith

Lindsay C. Days
ldays001@odu.edu

Duaa R. Alajroush
dalajrou@odu.edu

Khadija Faye
kfaye@odu.edu

Yara Khodour
ykhod001@odu.edu

*See next page for additional authors*

Follow this and additional works at: https://digitalcommons.odu.edu/chemistry_fac_pubs

Part of the Bioelectrical and Neuroengineering Commons, Cancer Biology Commons, and the Inorganic Chemistry Commons

Authors

Chloe B. Smith, Lindsay C. Days, Duaa R. Alajroush, Khadija Faye, Yara Khodour, Stephen J. Beebe, and Alvin Holder

DR. ALVIN HOLDER (Orcid ID : 0000-0001-9618-5297)

# SPECIAL ISSUE INVITED REVIEW

## Photodynamic Therapy of Inorganic Complexes for the Treatment of Cancer†

Chloe B. Smith,[1] Lindsay C. Days,[1] Duaa R. Alajroush,[1] Khadija Faye,[1] Yara Khodour,[1] Stephen J. Beebe,[2] and Alvin A. Holder[1]*

[1]Department of Chemistry and Biochemistry, Old Dominion University 4541 Hampton Boulevard, Norfolk, VA 23529, U.S.A.

[2]Frank Reidy Research Centre for Bioelectrics, Old Dominion University, 4211 Monarch Way, Suite 300, Norfolk, VA, 23508, U.S.A.

* Corresponding author email:   aholder@odu.edu  (Alvin A. Holder  )

†This article is part of a Special Issue dedicated to the memory of Dr. Karen Brewer

**Abbreviations:**

9-accm      1,7-(di-9-anthracene-1,6-heptadiene-3,5-dione)

AFM          Atomic force microscopy

AlTSPc        aluminium tetrasulfide phthalocyanines

an-tpy        4`-(9-anthracenyl)-2,2`:6`,2``-terpyridine

BODIPY        boron dipyrromethene

BPE          1,2-bis(4-pyridyl)ethane

bpy          2,2′-bipyridine

cat          benzene-1,2-diolate

Ce6          chlorin e6

dopa-NBD     4-(2-(4-nitrobenzo[c][1,2,5]oxadiazol-7-ylamino)ethyl)benzene-1,2-diolate

dpa          dipicolylamine

dpp          2,3-bis(2-pyridyl)pyrazine

dppz          dipyrido[3,2-*a*:2′,3′-*c*]phenazine

dpq          2,3-bis(2-pyridyl)quinoxaline

ER          endoplasmic reticulum

FPs          fine-sized particles

GQDs          graphene quantum dots

HAp          hydroxyapatite

HPV          human papillomavirus

HSA          human serum albumin

IP-nT          imidazo[4,5-f][1,10]phenanthroline

InTPP          tetraphenylporphyrin

MB          methylene blue

*m*TCPC        5,10,15-tris(*meta*-carbomethoxyphenyl)corrole

NPs          nano-sized particles

mPACT        photoactivated chemotherapeutic

pbt          2-(2'-pyridyl)benzothiazole)

| | |
|---|---|
| Pcs | phthalocyanines |
| phen | 1,10-phenanthroline |
| Ph$_2$phen | 4,7-diphenyl-1,10-phenanthroline |
| phen$_2$DTT | 1,4-bis(1,10-phenanthrolin-5-ylsulfanyl)butane-2,3-diol |
| ph-tpy | (4′-phenyl)-2,2′:6′,2″-terpyridine |
| pq | 3-phenylisoquinoline |
| PS | photosensitizer |
| *p*TCPC | 5,10,15-tris(*para*-carbomethoxyphenyl)corrole |
| PTT | photothermal therapy |
| PpIX | protoporphyrin IX |
| py-tpy | 4`-(1-pyrenyl)-2,2`:6`,2``-terpyridine |
| ROS | reactive oxygen species |
| salmet | *N*-salicylidene-*L*-methionate |
| sal-*L*-tryp | *N*-salicylidene-*L*-tryptophanate |
| SDT | sonodynamic therapy |
| Sil | silane arm |
| Stpy | (2,2′:6′,2″-terpyridin-4′-oxy)ethyl-β-D-glucopyranoside |
| tpphz | tetrapyrido[3,2-a:2`,3`-c:3``,2``-h:2```,3```-j]phenazine (tpphz) |
| tpy | 2,2′:6′,2″-terpyridine |
| TSPP | meso-tetra(4-sulfonatophenyl)porphyrin |
| ttpy | 4′-(p-tolyl)-2,2′:6′,2″-terpyridine |

**Abstract**

Photodynamic therapy (PDT) is a medicinal tool that uses a photosensitiser and a light source to treat several conditions, including cancer. PDT uses reactive oxygen species (ROS) such as cytotoxic singlet oxygen ($^1O_2$) to induce cell death in cancer cells. Chemotherapy has historically utilized the cytotoxic effects of many metals, especially transition-metal complexes. However, chemotherapy is a systemic treatment so all cells in a patient's body are exposed to the same cytotoxic effects. Transition metal complexes have also shown high cytotoxicity as PDT agents. PDT is a potential localized method for treating several cancer types by using inorganic complexes as photosensitizing agents. This review covers several *in vitro* and *in vivo* studies, as well as clinical trials that reported on the anti-cancer properties of inorganic pharmaceuticals used in PDT against different types of cancer.

## INTRODUCTION

Cancer is a major issue around the world given that the American Cancer Society recently reported that around 750,000 cancer cases were diagnosed in 2020 (1). In 2017, 2018, and 2019, the three most common causes of cancer related deaths in U.S. females were lung, breast, and colorectal cancers; while the most common causes of cancer related deaths in U.S. males were lung, prostate, and colorectal cancers (2-4). Declines in cancer incidence and death rates in the U.S.A. over the past decade have followed the national changes of cancer risk factors (e.g., excess body weight, decreases in human papillomavirus, and smoking) (5-8). Cancer screening, diagnostics, and treatments that include nanomaterials, inorganic pharmaceuticals, and PDT, have improved over the last few decades (9, 10).

PDT is a medically selective technique that has been widely used to treat different types of cancer and other diseases (11, 12). The effect of chemicals under light irradiation on cell death was discovered by Oscar Raab. He studied the interaction of light and acridine and showed a lethal effect on Infusoria (13). Shortly afterwards, the optical property of fluorescence was predicted to be potentially promising if used in medicine (14). The first medicine using the interaction between a fluorescent compound and light was used to treat skin cancer (15). PDT requires three fundamental components: a photosensitizer (PS), light, and molecular oxygen (16-18). When visible light is absorbed, the PS is promoted from the ground state up to the excited triplet state ($^3$PS) and can contribute to generating ROS ($^1O_2$, $^{\bullet}OH$, $H_2O_2$…) that selectively kill cancer cells (19-21). Photofrin is a PS that is currently being used as a PDT drug (22, 23). It stimulates the formation of cytotoxic $^1O_2$ species with red light (24, 25). Porphyrins have been evaluated in PDT because they strongly absorb light, which is then converted to energy and heat in cancer cells (26). Similarly, many metals and lanthanides can also be used as PSs to treat cancers (27). When these elements were used as non-PDT drugs, they showed anti-cancer activity, but also exhibited similar toxicity to other metal-based anti-cancer drugs. In addition, cancers treated with these elements also exhibit drug resistance (28). Toxic effects of metal-based complexes have evoked considerable interests to develop safer version of these drugs (29). Additionally, PDT reduces the toxicity of metal-based drugs on human organs compared to non-PDT chemotherapeutic drugs (30). There are various types of metal-based PDT anti-cancer drugs that have been reported recently (31-34). There has been increasing interest in the

development of light-activated metal complexes to exhibit photocytotoxicity through mechanisms independent of ROS production (35-38).

Light penetrates the tissue and excites a PS with a metal centre. This PS is then energetically promoted to $^3$PS, which can transfer electrons, protons, or emit light from this state. $^3$PS electron transfer typically interacts with cellular oxygen to form $^3O_2$ and $^3$PS proton transfer also interacts with cellular oxygen to form $^1O_2$. These resulting ROS can then lead to damages to DNA (39).

Based on the topic and PDT research as carried out by the late Professor Karen Brewer, it is fitting that the reader should read the following before proceeding to the selected metal centres that are utilised in PDT: the special Issue in *Inorganic Chimica Acta* on "*Coordination Chemistry: Understanding the role of molecular and supramolecular design on the photophysical, biological, and electron transfer properties of transition metal complexes and their potential applications. Dedicated to the memory of Karen J. Brewer*" (https://www.sciencedirect.com/journal/inorganica-chimica-acta/vol/454/suppl/C) and PDT chapters in the textbook entitled *"Ruthenium Complexes: Photochemical and Biomedical Applications"* (40-42).

This review will focus on the following metal centres, but with increasing atomic numbers of metals, starting with aluminium.

## ALUMINIUM

Aluminium-based complexes in combination with PDT have been reported to determine anti-cancer efficacy against melanoma skin cancer, non-melanoma skin cancer, and other diseases (43, 44). Phthalocyanines (Pcs) have been studied for their PDT potential due to their strong absorption at the red region of the spectrum (~670 nm), their excellent $^1O_2$ generation, their chemical stability, and effective tissue penetration (45). Pcs in conjunction with metals that are diamagnetic have been shown to have better sensitizing activity than metal-free Pcs (46). Aluminium phthalocyanine chloride (AlCPc) has been studied as a PDT agent as reported in the literature (47).

<Figure 1>

A murine model of non-melanoma skin carcinomas and normal skin was used to study the pharmacokinetics of the topical application of AlClPcA. This complex was not detected in normal

skin tissues, which indicates that the topical application of this solution does not lead to generalized toxicity or phototoxicity. Additionally, AlClPc penetrated the tumours of hairless mice 25 times more deeply than in normal skin. The results found that this complex can be a treatment option in the future for deep squamous cell carcinomas that cannot be treated by surgery (43).

Another study investigated cytotoxic effects of aluminium tetrasulfophthalocyanines (AlTSPc) in combination with PDT on melanoma skin cancer cells at different concentrations and compared the results to the cytotoxic effects in normal skin fibroblast and keratinocyte cells (44). Tetrasubstituted Pcs have high dipole moments and effective $^1O_2$ generation, making them ideal for combination treatment with PDT. This treatment did induce apoptosis in melanoma cells with symptoms such as protrusions in the plasma membrane and nuclear fragmentation and condensation. The results showed that 40 µg ml$^{-1}$ with low levels of light activation (4.5 J cm$^{-2}$) was effective in reducing the cell viability of melanoma skin cancer cells by inducing apoptosis, and this therapy has the potential to successfully treat melanoma skin cancer (44).

The topical administration of hydroxy-aluminium phthalocyanine (AlOH-PC) entrapped in liposomes was used for *in vivo* studies against human prostate carcinomas. The specific human prostate carcinoma cell lines, LNCaP and PC3 were utilized. The aggressive PC3 tumours had a 100% cure rate at a dose of 6 mg ml$^{-1}$, and the less aggressive LNCaP tumours had a 100% cure rate at 4.5 mg ml$^{-1}$. The results show that liposomal AlOH-PC prepared by a patented microfluidization procedure is potentially suitable for the PDT treatment of prostate carcinomas (48).

**TITANIUM**

Titanium oxide (TiO$_2$) has been used as a PS in PDT for cancer treatment due to its chemical stability, low toxicity, and high photocatalytic activity (49). *In vitro* study of carbon-doped TiO$_2$ (TiO$_2$:C) in X-ray-induced PDT was examined against A459 lung cancer cells and showed a significant toxicity compared to without X-ray irradiation. In addition, the *in vivo* study also confirmed a low A459 cancer cells viability by ROS generation. Overall, TiO$_2$:C inhibited cancer growth efficiently and improved PDT effects (50).

**VANADIUM**

Vanadium based complexes, especially oxovanadium complexes, have been known to exhibit anti-cancer properties as they have demonstrated the ability to induce apoptosis in cancer cells (51). This makes their use, a promising route to take in the fight against cancer, especially when combined with PDT. For instance, PDT activity was demonstrated by cell viability assay for the ternary oxovanadium(IV) complexes, shown in Fig. 2, [VO(salmet)(N-N)] and [VO(saltrp)(N-N)] (where N-N = phen, dpq, or dppz). This resulted in half maximal $IC_{50}$ values of $2.7 \pm 0.4$ mM and $2.5 \pm 0.2$ mM in MCF-7 (human breast carcinoma) and HeLa cells (human cervical cancer), respectively, in addition to efficient photoinduced DNA nuclease activity following two (2) hours exposure to blue (360 nm) and red (750 nm) lights (52).

Another oxovanadium(IV) complex, [VO(L$^2$)Cl$_2$], (where L$^2$ is N-(4-(5,5-difluoro-2,8-diiodo-1,3,7,9-tetramethyl-5H4Ⱪ4,5Ⱪ4-dipyrrolo[1,2-c:2′,1′-f][1,3,2]diazaborinin-10-yl)benzyl)-1-(pyridin-2-yl)-N-(pyridin-2-ylmethyl)methanamine), exhibited mitochondrial membrane disruption by JC-1 (1,1′,3,3′-tetraethyl5,5′,6,6′-tetrachloroimidacarbocyanine iodide) dye assay, in addition to $IC_{50}$ values of $0.15 \pm 2$ μM and $0.2 \pm 0.08$ μM in HeLa cells and MCF-7 cells, respectively (53). In another study, the PDT activity of the following oxovanadium(IV) complexes was determined: [VO(cat)(L)] and [VO(dopa-NBD)(L)], (where L is phtpy or stpy), shown in Fig. 2. Cytotoxic assays of these complexes, in the dark and in the presence of visible light of 400-700 nm and red light of 600-720 nm, showed that they exhibited increased toxicity against HeLa and Hep G2 cells, upon photoirradiation. These studies further confirm that the anti-cancer properties of vanadium are enhanced with the use of PDT when compared to in the dark (54).

<Figure 2>

**MANGANESE**

Manganese-containing complexes have been utilized in PDT due to their ability to increase the ROS level and Fenton reactions (55). Atif *et al.* synthesized and characterized $Mn_xCe_{1-x}O_2$ nanocomposites and analysed its anti-cancer properties against MCF-7 cells. When $Mn_xCe_{1-x}O_2$ nanocomposite was administered, apoptosis was observed in cells treated with 9% Mn-doped $CeO_2$

nanocomposites due to an increase in the production of ROS levels (56). A $Mn^{2+}$ ion and doxorubicin (Dox) were loaded onto an NP with phycocyanin (PC) to construct Mn nanococktails (PC-Mn@Dox-NPs). PC-Mn@Dox-NPs increased drug release rate and the generation of $H_2O_2$ and $^{\cdot}OH$ all leading to cytotoxicity (57).

A Mn complex was reported in combination with immunotherapy to heighten the combined therapeutic response. The $MnO_2$@Ce6 nanoprobes was tested *in vitro* and *in vivo* using human-induced pluripotent stem cells (iPSs) as a vehicle. The $MnO_2$ and $H_2O_2$ reversed the hypoxic tumour microenvironment, and after PDT, $^1O_2$ was generated alongside stimulation of an immune response (58).

**IRON**

Iron, when coordinated to certain ligands, has also shown cytotoxic abilities on cancer cells by causing DNA damage. Hence, making it important to investigate its potential effect on these cells when associated with PDT. Tabrizi *et al.* showed efficacy of mitochondria-targeted PDT with a Fe(II) complex containing BODIPY derivatives, [Fe(L)(tpy-BODIPY)], (with L being 5-methoxy-1,3-bis(1-methyl-1H-benzo[d]imidazol-2-yl)benzene), depicted in Fig. 3. This resulted in a $IC_{50}$ values of $1.05 \pm 0.3$ µM, against HeLa cells and $36.21 \pm 0.2$ µM, against noncancerous MRC-5 cells, in the presence of a light source with $\lambda = 500$ nm (59).

Another study by Sun *et al.* demonstrated the PDT activity of iron mono-hydroxyl metallocorrole complexes as shown in Fig. 3 in which each metal centre is coordinated by a corrole ligand, which is an aromatic macrocycle similar to corrin and porphyrin rings. Cytotoxic studies on A549 (human lung cancer), MCF-7, and HepG-2 cells after LED irradiation at $625 \pm 2$ nm resulted in relatively low $IC_{50}$ values of $18 \pm 3$ µM, $27 \pm 4$ µM, and $15 \pm 2$ µM respectively (60). These studies showed that iron complexes were suitable PDT candidates against cancer cells without being toxic to noncancerous GES-1 cells.

<Figure 3>

**COBALT**

Many studies have shown that cobalt-containing complexes can be used in PDT because they can photocleave DNA *in vitro* and bind to different chromophoric ligands and act as PSs (61, 62). For instance, the dark and light cytotoxicity of cobalt(III) curcumin complexes with different *N,N,N,N*-tripodal ligands (Fig. 4) were tested against DLD-1 colon cancer cells and MCF-7 cells to evaluate their PDT activity. The cobalt(III) complexes were nontoxic in the dark but accumulated in significant concentrations in the cell membrane. The cytotoxicity of the cobalt complexes exhibited around 20-fold increase when cells were treated with light (520 and 470 nm) for 15 min, whereas the photocytotoxicity of the free curcumin increased by only two-fold. The biological activity and strong stability of the cobalt-curcumin complexes were due to the nature of the ancillary ligand and cobalt reduction potential (63).

<Figure 4>

Two ternary cobalt(II) complexes, $[Co(9\text{-accm})(phen)_2](OAc)$ and $[Co(9\text{-accm})(dppz)_2](OAc)$, were synthesized to study their ability to kill cancer cells under visible light irradiation conditions. *In vitro* photoactivated cytotoxicity of the complexes were assessed in HeLa, MCF-7 and MDA-MB-231 (human breast cancer cell lines), and HPL1D (lung epithelial normal cells). The complexes showed low cytotoxicity in the dark, although in visible light, they could treat the cancer cells with low energy. The complexes showed a high photocytotoxicity in HeLa, MCF-7, and MDA-MB-231 cells by generating ROS, whereas they were non-toxic to the HPL1D cells. The high phototoxicity of the cobalt(II) complexes containing anthracene-based curcuminoid ligand make them suitable candidates for PDT (64).

Cobalt(II) complexes of terpyridine bases: $[Co(ph\text{-tpy})_2](ClO_4)_2$, $[Co(an\text{-tpy})_2](ClO_4)_2$, and $[Co(py\text{-tpy})_2](ClO_4)_2$ (Fig. 5) were prepared and their DNA photocleavage activity and photocytotoxicity on HeLa cells were studied. The photo-induced DNA cleavage activity of the complexes were carried out in UV-A light of 365 nm and visible light of 514 nm, 569 nm, and 647 nm. The an-tpy and py-tpy complexes at 2.5 µM concentration showed complete DNA cleavage activity in UV-A light, while the ph-tpy complex was inactive under similar light irradiation. Moreover, all complexes showed significant photocleavage activity in visible light due to the formation of $^1O_2$ and $^•OH$ species. According to the cytotoxicity property of the complexes under visible light, the an-tpy and py-tpy complexes showed a high PDT effect in HeLa cells giving $IC_{50}$

values of 24.2 and 7.6 µM, respectively. The authors concluded that these cobalt(II) complexes could be potent metal-based PDT agents (65).

<Figure 5>

In recent years, cobalt nanoparticles have been used as mediators for cancer treatment and drug delivery vehicles (66, 67). The photo-cytotoxic effect of $pCo_3O_4$ NPs was studied *in vitro* and *in vivo* against the murine breast cancer 4T1 cells. In case of *in vitro* study, the $pCo_3O_4$ NPs could kill cancer cells *via* inducing ROS and DNA damage after NIR irradiation at 808 nm without apparent side effects. The $pCo_3O_4$ NPs was injected into 4T1 cells in syngeneic BALB/c mice for *in vivo* study. This study showed a tumour necrosis under 808 nm irradiation. Moreover, $pCo_3O_4$ NPs exhibited broad near-infrared (NIR) laser absorbance, high photothermal conversion efficiency, distinguished colloidal stability, excellent biocompatibility, and promising multifunctional groups. Overall, $pCo_3O_4$ NPs represent a promising phototheranostics agent for multimodal imaging (photoacoustic/magnetic resonance imaging) and PTT/PDT synergistic phototherapy of tumours (68).

Park *et al.* synthesized multifunctional cobalt ferrite ($CoFe_2O_4$) NPs ($CoFe_2O_4$-HPs-FAs), where HP is hematoporphyrin and FA is folic acid. Photodynamic anti-cancer activity of $CoFe_2O_4$-HPs-FAs was investigated on FR positive (HeLa and KB) and FR-negative (MCF-7 and PC-3) cells. The $CoFe_2O_4$-HPs-FAs in FR-positive (Hela and KB) cells showed a slightly better photo-killing efficacy compared with the $CoFe_2O_4$-HPs-FAs in FR-negative (MCF-7 and PC-3) cells. The large amount of HP could generate high levels of $^1O_2$, which causes cell death during irradiation (69). Another study on $CoFe_2O_4$-HPs-FAs showed the photodynamic anti-cancer activity on prostate cancer PC-3 cells with FA according to the exposure dose of the green light-emitting diode (LED) light at doses of 3.06, 6.12, and 18.36 J cm$^{-2}$. The photo-killing efficacies of the $CoFe_2O_4$-HPs-FAs were markedly increased in a dose-dependent manner, and this is related to the close correlation between exposure dose of light and dose of the $CoFe_2O_4$-HPs-FAs (70).

## NICKEL

Nickel functions as an essential element in constructing enzyme cofactors, but it's biological role in humans still remains largely unknown (71, 72). Despite this, many researchers have recognized its role in PDT anti-cancer research. A nickel(II) porphyrin complex elicited

photonicking activity of circular plasmid DNA after administration (73). The potential relevance for eukaryotic DNA damage *via* photonicki,ng after PDT is worthy of investigation.

<Figure 6>

Another bifunctional nickel compound was investigated as a PS in PDT. This nickel chlorophyll derivative, methyl 3-devinyl-3-(1'-(benzyloxy)-ethyl)pheophorbide-a (Ni-PH-A), was investigated as a tumour imaging agent and PS. *In vitro* studies with MDAH-2774 (human ovarian endometrioid adenocarcinoma) cells and MCF-7 cells showed $IC_{50}$ values of 379.2 µM and 135.7 µM, respectively (74). *In vivo* studies also showed that the complex remained at a stable concentration in the lungs and liver. Concentration stability *in vivo* is a pharmacokinetic property associated with a greater PS character better suited for good treatment response (75).

**COPPER**

Copper is a nontoxic and bioessential element that is vital to the health of all living organisms, and therefore, photochemotherapeutic usage of different copper complexes is an interesting field of research (76, 77). The photodynamic activity of copper(II) complexes: $[Cu(L^1)B]ClO_4$ and $[Cu(L^2)B]ClO_4$ (where $L^1$ = 2-[(pyridin-2-yl)methyleneamino]phenol, $L^2$ = 2-[(pyridin-2-yl)methyleneamino]benzenethiol, and B are $^1$H-imidazo[4,5-f][1,10]phenanthroline) and 1-(pyren-2-yl)-$^1$H-imidazo[4,5-f][1,10]phenanthroline) was studied in a structure-activity relationship (SAR)-based approach. This study assessed the role of S-coordination to copper(II) in PDT on HeLa cells. The complexes exhibited toxicity in the dark with $IC_{50}$ values of ~10 µM. However, they showed a high toxicity in visible light with $IC_{50}$ values of ~1.0 µM due to $^1O_2$ generation. Overall, the S-coordination in modulating the *in vitro* photodynamic activity of the copper(II) complexes is crucial in designing copper-based next generation PDT agents (78).

<Figure 7>

The PDT effect of Cu-Try/MB NPs was studied *in vitro* against HeLa cells using a lactate dehydrogenase (LDH) cytotoxicity assay kit. The cells were irradiated with 650 nm laser (200 mW cm$^{-2}$) for 15 min. The Cu−Try NPs increased the ROS level to enhance the PDT efficacy and killed cancer cells effectively reaching to 71% cell death rate. *In vivo* experiment was studied against murine cervical cancer cells (U14) and showed an inhibition in tumour growth without effecting the other

normal organs. *In vitro* and *in vivo* studies indicated that enhanced PDT based on Cu−Try/MB NPs can reduce cancer cell viability (79).

## ZINC

Zinc is integral to many enzymes and transcription factors which control different fundamental cellular functions such as gene expression, DNA replication, DNA repair, and apoptosis (80). A large number of zinc complexes showed *in vitro* photocytotoxicity against different human cancer cell lines. A study by Nene *et al.* reported the *in vitro* PDT activity of two morpholine-substituted Zn(II) Pcs conjugated to graphene quantum dots (GQDs) and biotinylated GQDs (GQDs-biotin) by non-covalent π-π interactions. The PDT activities of GQDs with biotin was increased due to improved drug uptake in the Pcs-GQDs-biotin conjugates, where the cell viability was 34.9% after treatment. In addition, the cell viability was decreased from 66.2% to 51.2% after treatment with 4-GQDs and 5-GQDs, respectively. Overall, the GQDs, cationic charges, and biotin transport helped to improve the therapeutic efficacy of Pcs *in vitro* during PDT by improving the concentration of Pcs penetrating the cells (81).

Many studies have demonstrated that zinc-porphyrins have a high therapeutic effect on cancer cells (82). Pan *et al.* developed three Meso-substituted porphyrins with zinc molecules: 5,10,15,20-tetrakis(3,4-bis(2-(-2-(2-hydroxyethoxy)ethoxy)ethoxy)benzyl) zinc porphyrin (P1), 5,15-bis(3,4-bis(2-(-2-(2-hydroxyethoxy)ethoxy)ethoxy)benzyl)- 10,20-bis(2-(2-(4-ethynylphenoxy)ethoxy)ethoxy)ethanol) zinc porphyrin (P2), and 5,15-bis(3,4-bis(2-(-2-(2-hydroxyethoxy)ethoxy)ethoxy)benzyl)-10,20-N,N-dibutyl-4-ethynylaniline zinc porphyrin (P3), (Fig. 8). They studied the photodynamic activities of zinc porphyrins (P1-P3) against HeLa cells after illumination (650 nm, 40 mW cm$^{-2}$) for 10 min. All Zn-porphyrin compounds presented a decent biocompatibility and marvellous photocytotoxicity giving IC$_{50}$ values from 5 μM to 7 μM. The compounds showed a high percentage of cell death due to their strong π-π interactions within porphyrin molecules. The authors suggested that all these Zn-porphyrins had the promising potential in PDT for cancer (83).

**<Figure 8>**

Another example of PDT with zinc-porphyrins demonstrated that the 5,10,15-tris (phenyl)-20-[4-(2-(2-methyl-5-nitro-imidazolyl)ethoxyl)phenyl]porphyrin ($H_2Pp$) and its zinc(II) metalloporphyrin (ZnPp) complex (Fig. 9) exhibited very low cytotoxicity towards breast cancer cells in the dark with the survival rate above 80%. However, after UV irradiation for 30 min, the cell survival rate with $H_2Pp$ and ZnPp was decreased to 65.3% and 17.8%, respectively. The anti-cancer activity of the zinc(II) porphyrin was much higher than that of the free porphyrin ($H_2Pp$). Overall, ZnPp complex showed a significant PDT effects for treating breast cancer (84).

<Figure 9>

## MOLYBDENUM

NPs from octahedral molybdenum cluster compound $(n-Bu_4N)_2[Mo_6I_8(OCOCF_3)_6]$ were reported to be radiosensitizers for X-ray induced PDT. The cytotoxic effect of the NPs on HeLa cells was first examined under UVA/blue-light irradiation in order to demonstrate the biological effects of photosensitized $O_2(^1\Delta g)$. In the dark, the molybdenum NPs were not toxic at physiologically relevant concentrations up to 15 µM. However, the cell viability decreased under 460 nm light. There was strong phototoxicity in the nanomolar concentration range (85).

Brandhomeur *et al.* prepared poly (*D,L*-lactide-co-glycolide) (PLGA) NPs embedding inorganic molybdenum octahedral cluster to evaluate its anti-cancer properties in PDT. Tetrabutylammonium salt of $[Mo_6Br_{14}]^{2-}$, $(TBA)_2Mo_6Br_{14}$ cluster compound loaded PLGA nanoparticles (CNPs) was prepared. *In vitro* cell viability studies were carried out on A2780 (ovarian cancer) cells treated with clusters or CNPs. The results in dark did not show any sign of toxicity in concentrations up to 20 µg/ml. In case of the photo-activation test at 365 nm, CNPs were able to reduce the cell viability up to 50% and generate $^1O_2$. The authors concluded that $(TBA)_2Mo_6Br_{14}$ can be used as an efficient PS for PDT and PLGA NPs as an effective delivery system against cancer cells (86).

## RUTHENIUM

Ruthenium complexes make great candidates for PDT due to their efficient $^1O_2$ generation (87), their abundant visible light absorption (88), their therapeutic abilities, and their ability to

photocleave DNA (89, 90). Ruthenium complexes also have strong two-photon absorbing and luminescence properties (91). Though Ruthenium complexes have very promising anti-cancer and PS properties, their cell selectivity is lacking. Ru(II) polypyridyl complexes have this problem which leads to normal cells experiencing the cytotoxic effects instead of the cancer cells. The antiestrogenic breast cancer treatment drug, Tamoxifen, competes with and binds to ER, ultimately leading to programmed cell death. An ER targeting Ru(II) polypyridyl complex (Ru-tmxf) was synthesized in order to target and treat breast cancer with two-photon PDT (92).

<Figure 10>

<Figure 11>

The suitability of Ru-OMe and Ru-tmxf was tested with a maximum two-photon action cross-sections estimated to be 160-180 Göppert-Mayer units at 820-830 nm. The cytotoxicity and cellular uptake of these two complexes were tested with MCF-7 cells (ER+ breast cancer cells) and MDA-MB-231 (ER- breast cancer cells). In dark conditions, both Ru-tmxf and Ru-OMe had little cytotoxicity, but upon irradiation, Ru-tmxf (16 µM) resulted in 99% cell death. While Ru-OMe only had a 17% cell death for MCF-7 cells under the same conditions. Ru-tmxf could generate $^1O_2$ effectively under TP irradiation. It was proven that Ru-tmxf is an ER-targeting Ru(II) polypyridyl PS that is an excellent candidate for PDT for breast cancer. The first functional subunit of this compound, tamoxifen, efficiently targets the ERs on ER+ breast cancer cells. The other subunit of the compound, a Ru(II) polypyridyl PS that acted as a two-photon fluorescence probe, that can be used for tracking cellular uptake and location, and as a two-photon excited $^1O_2$-generating PS. Ru-tmxf treats ER+ breast cancer by selectively damaging lysosomes in ER+ breast cancer cells. This makes Ru-tmxf a great potential ER+ breast cancer PDT treatment (93).

Ruthenium complexes have also been studied to treat malignant melanoma. Two novel mixed-metal binuclear complexes that contain a ruthenium(II) PS and a vanadium(IV) metal centre, of which have terminal and bridging polypyridyl ligands. Ruthenium and vanadium were chosen due to their anti-cancer properties and their ability to photocleave DNA. Complexes 2, 3, 4, and 5 were synthesized and characterized; then utilised as PDT agents.

<Figure 12>

<Figure 13>

The cell lines used in these studies are A431 (human epidermoid carcinoma), amelanotic malignant melanoma, and non-cancerous HFF (human skin fibroblast) cells. A431 and HFF non-cancerous cells demonstrated the greatest difference in inhibition of cell proliferation. [Ru (pbt)$_2$(phen$_2$DTT)VO(sal-$L$-tryp)]Cl$_2$ and [Ru(pbt)$_2$(tpphz)VO(sal-$L$-tryp)]Cl$_2$ had the strongest efficacy in inhibiting melanoma cell growth when compared to Na$_4$[Co(tspc)(H$_2$O)$_2$] in both dark and light studies (94).

Ruthenium complexes of polyazine ligands have interesting redox and photophysical properties. Mixed-metal supramolecular complexes containing ruthenium have been studied for their ability to photocleave DNA upon irradiation with visible light. Complexes such as [((bpy)$_2$Ru(dpp))$_2$RhCl$_2$](PF$_6$)$_5$, [((bpy)$_2$Os(dpp))$_2$RhCl$_2$](PF$_6$)$_5$, and [((tpy)RuCl(dpp))$_2$RhCl$_2$](PF$_6$)$_3$, have been studied for their metal-to-ligand charge transfer (MLCT) based transitions and their metal-to-metal charge transfer (MMCT) excited states (95, 96). The supramolecular complexes listed above with low lying MMCT states can photocleave when excited into their intense MLCT transitions (97, 98). The photoactivity of the Ru(II) complexes was also reported to be regulated by the induction of distortion into the octahedral geometry around the metal. Ruthenium polypyridyl complexes have been shown to induce $^1$O$_2$-mediated DNA photocleavage when exposed to UV or visible light (99). Some ruthenium agents have also been reported to be able to act in hypoxic tissues *via* O$_2$-independent mechanisms (100). Complexes with these properties that can photocleave DNA, and complexes that can function as a photosensitizer are useful to developing PDT.

The mononuclear polyazine complexes, [(Ph$_2$phen)$_2$Ru(dpp)]$^{2+}$ and [(Ph$_2$phen)$_2$Os(dpp)]$^{2+}$ (Ph$_2$phen = 4,7-diphenyl-1,10-phenanthroline; dpp = 2,3-bis(2-pyridyl)pyrazine) were synthesized and investigated for the PDT treatment of cancer. Their efficacies as light activated anti-cancer drugs were tested against F98 cells (malignant rat glioma cells). Upon irradiation with blue light, these compounds presented excellent phototoxicity, but in the dark, they had negligible cytotoxicity. The IC$_{50}$ value of the complex in red light (625nm) [(Ph$_2$phen)$_2$Os(dpp)]$^{2+}$ was (86.07 ± 8.48) μM (101).

Graphene, single-walled carbon nanotubes (SWCNTs), single wall carbon nanohorns (SWCNHs), and other carbon nanomaterials have become increasingly popular for photothermal therapy (PTT) as excellent drug delivery devices. SWCNTs have been proven to induce cell death

with PTT, and future studies with them can develop multimodal therapies to combine PTT and PDT. Ruthenium was chosen for combination therapy with carbon nanotubes because of its anti-cancer properties and efficient $^1O_2$ generation. The Ru@SWCNHs were synthesized by sonicating complexes 6 and 7 with SWCNTs solutions for four hours at room temperature. This was repeatedly washed to remove free Ru(II) complexes. The Ru@SWCNTs were dispersed in an aqueous solution because they are not water-soluble.

<Figure 15>

The cytotoxicity of Ru@SWCNTs, SWCNTs, and Ru(II) complexes was tested against HeLa cells. When tested with only the Ru@SWCNTs, there was negligible toxicity, and when tested with only the laser there was negligible toxicity as well. The results showed that, with the laser, the Ru@SWCNTs were much more effective at killing the cancer cells than the SWCNTs and the Ru(II) complexes alone. When tested against multicellular tumour spheroids (MCTSs), Ru@SWCNTs exhibited excellent bimodal PTT and PDT effect. The efficacy of the Ru@SWCNTs was also tested *in vivo* on nude mice bearing HeLa tumours. After 15 days of observation, the Ru@SWCNTs, with the laser therapy, showed gradual shrinking of the tumours or even disappearance without regrowth. The laser alone or Ru@SWCNTs alone treatment resulted in rapid tumour growth after 15 days. Overall, Ru@SWCNTs in combination with PTT and two photon PDT was a successful bimodal anti-cancer therapy. *In vivo* and *in vitro* studies showed that Ru@SWCNTs successfully produced $^1O_2$ upon 808 nm diode laser irradiation, and has high efficacy as a PDT and PTT combination therapy to treat cancer (102, 103).

<Figure 16>

A study by Paul *et al.* reported the synthesis of ruthenium(II) conjugates of boron-dipyrromethene and biotin for targeted PDT in red light. The ruthenium(II) complexes of NNN-donor dpa bases having BODIPY moieties, were prepared and characterized by spectroscopic techniques and their cellular localization/uptake and photocytotoxicity studied. The photocytotoxicity assay of the complexes was examined against A549 and HPL1D cells. The complexes were basically nontoxic in the dark. In the visible light, the complexes had IC$_{50}$ values of ~2.0 and 0.98 μM in A549 cells. The photocytotoxicity of the complexes was reduced by ~4-fold in the HPL1Dcell line (104).

TLD1433 complex has been tested against numerous cancerous cell lines and has proven to have efficacious anti-cancer activity. Since this complex has a light-absorbing metallic scaffold and shows dual type I/type II photo-reactivity, it can generate enough radicals and $^1O_2$ species to cause cancerous cell death (105).

A study aimed to discover if TLD1433 could be activated by an optical surface applicator (OSA) for the intra-operative PDT of non-small cell lung cancer A549 cells. The results of the TLD1433-mediated PDT with 532 nm and 630 nm of light proved an $EC_{50}$ value of 1.98 μM (J cm$^{-2}$) and 4807 μM (J cm$^{-2}$) for green and red light, respectively. It was also shown that > 20 J cm$^{-2}$ of 532 nm light from the OSA was delivered to places with 100% loss of cell viability. The results show that TLD1433 activated by an OSA is a potential treatment for lung cancer (106).

TLD1433 was also tested to determine its anti-cancer efficacy against bladder cancer and conjunctival melanoma (107, 108). TLD1433 was tested *in vitro* and *in vivo* against AY-27, rat urothelial derived tumour cells, and T24 human bladder carcinoma cells. The *in vitro* studies exhibited high efficacy against the T24 and AY-27 cancer cells. For the *iv vivo* studies, the calculated $LD_{50}$ values as a function of absorbed photon density were shown to be 1.14 x $10^{16}$ and 8.17 x $10^{16}$ hv cm$^{-3}$ for T24 cells and 5.7 x $10^{15}$ and 2.71 x $10^{16}$ hv cm$^{-3}$ for AY-27 cells with green and red activation wavelength, respectively. The $LD_{50}$ value is significantly lower than that of Photofrin proving that TLD1433 has excellent phototoxicity. Also, enhanced bladder uptake of the complex and tumour necrosis was detected close to 1.5 mm in depth in the bladder. PDT treatment with TLD1433 in non-muscle invasive bladder cancer showed to be a selective and effective cancer treatment (108).

TLD1433 was tested against multiple cell lines, conjunctival melanoma (CRMM1, CRMM2, and CM2005), uveal melanoma (OMM1, OMM2.5, and MEL270), epidermoid carcinoma (A431), and cutaneous melanoma (A375). Apoptosis and necrosis of these cells was detected after treatment with TLD1433 and 15 minutes of green light irradiation (21 mW cm$^{-2}$, 19 J cm$^{-2}$, 520 nm). Further testing was conducted where CRMM1 and CRMM2 cells were injected behind the eye (orthotopic) or into the circulation of the fish (ectopic). The fish were then incubated in water containing TLD1433, injected with TLD1433 intravenously, or injected with TLD1433 retro-orbitally. The non-toxic PDT protocol used on the fish was four treatments of 90 minutes of green light irradiation (21 mW cm$^{-2}$, 114 J cm$^{-2}$, 520 nm) and 60 minutes drug-to-light intervals. Results showed that TLD1433 inhibited

tumour growth in the orthotopic fish when treated retro-orbitally. It also inhibited tumour growth in the ectopic fish when treated intravenously or retro-orbitally. The incubation in water treatment was too phototoxic to yield good results. Overall, TLD1433 exhibited excellent anti-cancer properties *in vivo* against cutaneous melanoma cells (107).

## RHODIUM

Rhodium complexes bind to DNA in a similar way to cisplatin and have also been studied for their PDT effects (109). Rhodium NPs have been studied over the years as novel photosensitizing agents in PDT for cancer treatment (110). The photodynamic effect of the RhNPs was studied *in vitro* on HeLa cells with and without NIR radiation (800 nm, 2.5 W $cm^{-2}$ and 10 min). The cell viability decreased significantly at concentrations over 5 mg $L^{-1}$ with NIR radiation. The effect of NIR exposure on HeLa cells was negligible and could be safely used for PDT in a wide concentration range (from 0.1 to 10 mg $L^{-1}$) (111).

Another study on RhNPs reported the development of rhodium-based (mesoporous polydopamine) NPs and PS chlorine6 (Ce6-Rh@MPDA). This study examined the photodynamic effects of these synthesized RhNPs on 4T1 cells which were irradiated with a 635 nm laser for 10 min. The phototoxicity of Ce6-Rh@MPDA was increased in a dose-dependent manner due to the presence of MPDAwhich improved the catalytic RhNPs efficiency (112).

## PALLADIUM

Palladium has no biological role in humans, and many studies went underway to compare Pd complexes and their anti-cancer properties to Pt complexes. However, Pd often decomposed into $Pd^{2+}$ during experiments (113). Recently, Pd particles between 0.25-0.5 µm were reported to induce DNA adducts in A549 cells (114). A series of palladium complexes were investigated as PSs in PDT against HeLa cells. Tripor and Pd-Tripor $IC_{50}$ values after PDT were 18.2 µM and 9.6 µM, respectively (115). These low $IC_{50}$ values indicate that Pd has anti-cancer properties when effective ligands are coordinated to the metal (116).

A binuclear species, Pd, Pt PS, Pd@Pt-PEG-Ce6, was reported to address the requirements of a PS entering a solid hypoxic tumour microenvironment. In this specific microenvironment, a typical PS is ineffective because they are hydrophobic and rely on oxygen-dependent reactions. Wei and co-

workers designed a novel bimetallic Pd, Pt PS with reduced hydrophobicity and better tumour selectivity than that of previously reported PSs. Pd@Pt-PEG-Ce6 and Pd@Pt in *vitro* biocompatibility and cytotoxicity after PDT in 4T1 and HeLa cells was observed *via* $^1O_2$ generation. Confocal fluorescence imaging and flow cytometry showed cellular localization, which confirmed biocompatibility. *In vivo* studies in 4T1 subcutaneous tumour mouse models showed that Pd@Pt-PEG-Ce6 had a long blood circulation time after PDT treatment (117).

**SILVER**

Silver NPs are commonly used in combination with PDT for the treatment of certain cancers. They have been extensively studied for their anti-tumour properties and ability to induce apoptotic cell death (118). The cytotoxicity of Ag NPs was tested against A549 cells using comet assay and single cell gel electrophoresis was used to determine DNA damage. This study proved that the enhanced cytotoxicity of the Ag NPs in combination with PDT was due to the increased intracellular ROS. The Ag NPs used in this experiment were spherical in shape and 27 nm in size, which is preferable as cytotoxicity is dependent on the size of the Ag NPs. This combination with PDT also showed significant DNA fragmentation when compared to the control group where p < 0.0001. The exact pathway by which Ag NPs enhanced cytotoxicity is not known, but it could be caused either by post oxidative stress occurring upon ROS generation and DNA fragmentation, or the generation of ROS by silver ions causing DNA fragmentation (119).

Ag NPs have also been tested in combination with PDT against B16F10 (skin melanoma) and A431 cells and this resulted in a maximum inhibition of 68.11% and 76.70% in 1 mM concentration, respectively. Upon combination with 5-aminolevulinic acid (5-ALA), an inhibition of 81.01% at 1mM concentration on A431 cells was obtained. When used with PDT, 5-ALA-silver nanoparticle conjugates resulted in lower $IC_{50}$ values than Ag NPs against both B16F10 and A431 cells, which shows that 5-ALA-silver nanoparticle conjugates had better anti-cancer activity than pure Ag NPs and 5-ALA alone. This experiment showed that at physiological pH, 5-ALA could effectively bind to positively charged Ag NPs through electrostatic interaction, and combination of this treatment with PDT can be used for the selective destruction of carcinoma cells (120).

Silver nanoparticles and nanoclusters have also been tested against MCF-7 cells. Ag NPs were extracted from the *Cynara scolymus* (artichoke) using microwave irradiation. These Ag NPs where

spherical and 200-223 nm average diameters. The $IC_{50}$ value of the Ag NPs with PDT was determined to be 10 mg ml$^{-1}$. The green synthesized Ag NPs with PDT therapy showed efficient anti-cancer activities *via* mitochondrial apoptosis in MCF-7 cells. The intrinsic apoptosis pathway was induced by Ag NPs and PDT combination therapy through up-regulation of pro-apoptotic proteins of the Bax and downregulation of the anti-apoptotic proteins Bcl-2 in MCF-7 cells (121).

Another study used bovine serum albumin protein-templated silver nanoclusters (BSA-Ag$_{13}$), which has 13 silver atoms per cluster, and studied their cytotoxic effects against MCF-7 cells. The measured $IC_{50}$ value for BSA-Ag$_{13}$ with PDT is 50 μM. The PDT in this experiment involved irradiating the cells with a 150 mW white light source, and the cell viability was measured with a MTT assay. MCF-7 cells were effectively killed upon NC uptake and white light treatment, demonstrating the good potential of BSA-Ag$_{13}$ NC in cancer treatment *via* PDT (122).

**INDIUM**

Indium complexes increase the *in vitro* and *in vivo* photodynamic efficacy more than Photofrin due to their high effectivity in the photooxidation of red blood cells when located in the core of the PS structure (123). The photodynamic activity of Indium(III)-meso-InTPP, which was encapsulated into NPs of poly(D,L-lactide-co-glycolide) (PLGA), was studied against prostate cancer cells (LNCaP) with incident light dose (15–45 J cm$^{-2}$), in comparison with the free InTPP. The InTPP-loaded NPs were more effective than the free drug, resulting in the reduction of cell viability. Encapsulated InTPP was three times more internalized into the cells than the free InTPP. The photocytotoxic effect of NPs loaded with InTPP showed high potential as a PDT agent due to their ability to generate $^1O_2$ (124).

**TIN**

The phototoxicity of Tin ethyl etiopurpurin (SnET2) was examined against canine prostates in adult male mongrel dogs in a series of four studies. SnET2 in combination with transurethral and transperineal light resulted in an average prostate tissue volume decrease of 52% (125). These results suggest promising implications for future clinical trials with this treatment plan. Another anti-cancer PS was investigated and found to have antimetastatic properties. β-SnWO$_4$ nanoparticle photocatalyst was reported in *in vitro* and *in vivo* studies. HepG2 cells showed ROS-induced

apoptosis and necrosis with an $LD_{50}$ of $< 0.5$ μM (126). This low $LD_{50}$ value unveils the excellent anti-cancer efficacy of this PS.

A multimodal bimetallic NP complex, Fe@Sn-UCNPs, was reported as endogenous $H_2O_2$-activatable, generating $O_2$ through catalytic reaction, and exhibiting photothermal performance (127). Tumour hypoxia differentiates tumour tissue from surrounding tissue and characteristic of poor prognosis in some cases (128, 129). Designing a PS independent of $O_2$ concentration is an important development in PDT options for patients with different tumour microenvironments. Additionally, the treatment modality is flexible with this PS, which is another important development for multiple types of cancer patients seeking treatment. Elevated tumour $O_2$ levels enhanced PDT effects *in vitro* and *in vivo*. *In vitro* phototherapeutic effects of Fe@Sn-UCNPs, magnetic Fe@Sn-UCNPs, and magnetic Fe@Sn-UCNPs showed sufficient phototoxicity (127). Multifunctional PSs are the most efficient PDT agents and emphasize cost efficacy for future administration to patients. Therefore, this PS offers many advancements to anti-cancer PDT.

**HAFNIUM**

Hafnium oxide NPs have a high electron density where they can generate a large number of electrons in tumour cells (130, 131). The photodynamic activity of hafnium-doped hydroxyapatite (Hf:HAp) NPs was studied under ionizing radiation against A549 lung cancer cell line using *in vitro* and *in vivo* models. The cytotoxicity (LDH) assay showed damage in the cells related to the formation of ROS. The *in vivo* studies demonstrated that the Hf:HAp NPs, with ionizing radiation, caused an inhibition in the tumour growth by apoptosis. Overall, the potential of Hf:HAp NPs can be used in a palliative treatment after lung surgical procedure (132).

**TUNGSTEN**

Tungsten oxide (WO$_3$-x/Dpa-Mel) NPs have phototherapeutic activity under 980 nm laser, but that causes unfavourable heating effect on normal tissues (133, 134). A study reported the synthesis of a novel dopamine enveloped WO$_3$-x/Dpa-Mel NPs to achieve a PDT effect on solid tumours under single 808 nm of NIR laser irradiation, avoid overheating, and obtain deep tissue penetration. *In vitro* phototoxic activity of WO$_3$-x/Dpa-Mel NPs was studied against 4T1, HeLa and MDA-MB-231 cells. The excellent PDT effect and stability of WO$_3$-x/Dpa-Mel NPs was confirmed under the 808 nm laser

irradiation. Additionally, *in vivo* application was examined on male BALB/c mice bearing subcutaneous 4T1 murine breast cancer tumours to evaluate PDT of $WO_3$-x/Dpa-Mel NPs. The results showed that $WO_3$-x/Dpa-Mel NPs can create an excellent synergistic phototherapy effect on solid tumour ablation *in vivo* without damaging healthy tissues under the light irradiation (135).

Other tungsten NPs like FA-WN-Ce6 (FWC) NPs, were synthesized to evaluate PDT effect against hypoxic tumours using *in vitro* and *in vivo* models. FWC NPs could selectively accumulate in tumour sites under 630 nm laser irradiation to form oxygen, which increases ROS generation. The phototoxicity of FWC NPs was evaluated on COS7 (normal mouse fibroblast) and CT26 (colon carcinoma) cell lines, and free Ce6 was chosen as the control. A high concentration of cell death (70%) was showed in CT26 cells when they incubated with Ce6 at a concentration of 4 $\mu$g $ml^{-1}$ in normoxia, while around only 40% cells were killed when the $O_2$ level was 1%. In contrast, the cell viabilities for FWC NPs were less than 30% in both normoxia and hypoxia at the same Ce6 concentration (4 $\mu$g $ml^{-1}$). To conclude, FWC NPs could have an excellent PDT effect in hypoxic tumour tissues (136).

## RHENIUM

Rhenium compounds have been investigated to determine their photocytotoxic behaviour against cancer cells (137). A study by Einrem *et al.* reported the synthesis of a set of rhenium(V)-oxo meso-triarylcorroles bearing ester and carboxylic acid functionalities. The two carboxylic acids Re[*m*TCPC](O) and Re[*p*TCPC](O) were used to study the phototoxic/cytotoxic effects on rat bladder cancer cells (AY27) and human colon carcinoma cells (WiDr). Both isomeric complexes induced 50% cell death after about 5 min of blue light exposure (435 nm, 0−40 min) on the AY27 cell line. Whereas, the meta-isomer was more active, effecting around 50% cell death in 8 min, and the para-isomer achieved about 50% cell death in 12 min on the WiDr cells (138).

Dinuclear phosphorescent rhenium(I) complexes: $[(L^1)(CO)_3Re(BPE)Re(CO)_3(L^1)](PF_6)_2$ (DRe1) and $[(L^2)(CO)_3Re(BPE)Re(CO)_3(L^2)](PF_6)_2$ (Dre2), where $L^1$ is 1-(pyridin-2-yl)-9H-pyrido[3,4-b]indole and $L^2$ is 1-(quinolin-2-yl)-9H-pyrido[3,4-b]indole were synthesized to survey their PDT effects. The photodynamic activity of the dinuclear Re(I) complexes was tested *in vitro* against A549 cells upon visible light of 425 nm for 15 min. The complexes Dre1 and Dre2 showed a significant photocytotoxicity toward A549 cell lines giving $IC_{50}$ values of 0.26 and 0.11$\mu$M,

respectively compared to 8.3μM for cisplatin. The authors suggested that these complexes may be used as potential anti-cancer and PDT agents (139).

**OSMIUM**

Osmium is an excellent element to use for PDT because it offers a characteristic unlike most elements, which is panchromatic absorption. Panchromatic absorption is an ideal characteristic for a PS because so many, if not all, wavelengths of light will activate its phototoxic effects. Panchromatic PSs can broaden the therapeutic window of activatable light wavelengths. A bimetallic $Os^{II}$, $Pt^{II}$ complex was reported to bind to DNA and reduce DNA migration better than cisplatin (140). In the presence of Pt, Os can function as a DNA binding agent, enhancing the DNA binding properties of Pt alone, which can greatly impact the field of cancer treatments.

$[((bpy)_2Os(dpp))_2RhCl_2](PF_6)_5$ was reported as a photocleaving PDT agent against DNA (105). The binuclear complex, $[((bpy)_2Os(dpp))_2RhCl_2]Cl_5$, was found to be phototoxic against Vero cells at a wavelength below the typical range that is considered therapeutic for PDT. The trinuclear complex was only cytotoxic after light exposure, which displayed photoactivity that could lead to enhancing PDT in future studies (96).

A mononuclear Os(II) complex $[(Ph_2phen)_2Os(dpp)]^{2+}$, elicited a phototoxic effect in response to blue light PDT against rat glioma F98 cells. In addition, $[(Ph_2phen)_2Os(dpp)]^{2+}$ showed cytotoxicity under the therapeutic window of light used in PDT. The broad range of photoactivity unveils promising developments in cancer treatment. The complex's cytotoxicity was remarkably higher than that of cisplatin, presenting a promising new PDT agent that is more effective than current chemotherapy options (101).

Four osmium-based PSs were reportedly synthesized, characterized, and evaluated for their phototoxicity in PDT. An Os(phen)$_2$-based scaffold was added to a series of IP-nT ligands tethered to n = 0–4 thiophene rings. $[Os(phen)_3]Cl_2$, Os-0T, Os-1T, Os-2T, Os-3T, Os-4T were described in the study and used in *in vitro* experiments to reveal that Os-4T produced the lowest half minimal effective concentration ($EC_{50}$) value amongst the rest of the PSs in the series. Os-4T also showed an impressive $EC_{50}$ value in both hypoxic and normoxic conditions, were 0.651 μM and 0.803 μM, respectively (141). This indicates Os-4T could be similarly effective in tumours with variable

oxygen content. Other studies showed that the complex, Os-4T, would be a wonderful candidate for more *in vivo* studies because mice tolerated the high maximum dose.

Lazic *et al.* synthesized, characterized, and assessed the biological activity of a series of new osmium-based PSs, TLD1822, TLD1824 and TLD1829. The PSs were activated in a fantastically broad spectrum of light during PDT *in vitro* and *in vivo* experiments with the complexes. Their wide range of photoactivation and cytotoxicity enables the PSs to have the best treatment flexibility compared to other elements. It also creates promising implications for increasing PS efficacy. *In vivo* studies of TLD1829 PS showed that the complex could treat colon cancer in mice (142). TLD1829 could have the potential to become a PDT agent used in colon cancer treatments.

An osmium(II) complex $[Os(bpy)_2 (IP-4T)](PF_6)_2$ was reported to be a promising anti-cancer PDT agent after NIR irradiation. *In vitro* experiments in MCF-7 cells showed that the complex was localized within the cytoplasm. A patent of a cancer vaccine was reported. The vaccine included inactivated cancer cells treated with an Os complex, PDT, and electromagnetic radiation. The components of the vaccine were reported as effective in prompting an immune response, which contributed to the field of cancer immunotherapy (143). This invention has established anti-cancer PDT's role in forwarding the progress of anti-cancer immunotherapy.

A novel Os(II) complex (Os1) was synthesized alongside a Ru(II) (Ru1) analogue to compare their phototoxicities. In vitro studies were conducted with Os1 and Ru1 in A549 cells. Os1 was excited by 700-850 nm, and Ru1 was excited by 550-700 nm. Both Ru1 and Os1 exhibited photostability. Os1 was localized in lysosomes while Ru1 was localized in mitochondria. Os1 also showed better multifunctional PS activity as a PDT agent and imaging agent (144). This study further shows the capabilities of Os as a PDT agent, which can be multifunctional and photostable. These are important characteristics that describe quality PSs.

## IRIDIUM

A series of Ir(III) complexes that targeted the endoplasmic reticulum (ER) redox signalling pathway to induce apoptosis were reported. All complexes migrated into the ER and induced apoptosis in A549 cells. The complex Ir2 was the most cytotoxic with an $IC_{50}$ value of 0.65 μM. Low $IC_{50}$ values enable complexes to perform well as PSs in the future by reducing any exposure related

toxicity in future *in vivo* studies or clinical trials. This PS has promising results for the future of PDT (145).

Another Ir(III) complex, [Ir(ttpy)(pq)Cl]PF$_6$, was developed and utilized photoredox catalysis to have a phototoxic effect independent of oxygen presence. The PDT reaction occurring in hypoxic conditions is a remarkable advance in the field of PDT treating cancer. The tumour microenvironment is often variable from one tumour to the next, and this includes oxygen presence. Utilizing a cytotoxic mechanism independent of this variable can increase the availability of this PS option in patients in the future. This capability has promising implications for further PDT advancements (146).

An Ir(III) complex with the ligand (4,15-bis[4-(N,N-diphenylamino)phenyl][1,2,5]thiadiazolo-[3,4-i]dipyrido[a,c]phenazine) was reported as a highly efficient ROS generator, with negligible dark toxicity. The complex was administered in *in vitro* and *in vivo* experiments and showed photostability and cytotoxicity under 808 nm irradiation. This complex utilized aggregation-induced ROS generation, which is a unique method of ROS generation for PSs (147). This Ir complex introduced a unique role as a highly efficient anti-cancer PDT agent.

A cyclometallated [Ir(ppy)$_2$(L$^1$)][PF$_6$], where L$^1$ = fluorenyl 5-substituted-phen, was reported as a future photosensitiser in two-photon excited photodynamic therapy. [Ir(ppy)$_2$(L$^1$)][PF$_6$] photocytotoxicity was tested against C6 Glioma (malignant nervous) cells and produced $^1$O$_2$ at 740 nm (148).

## PLATINUM

Platinum-based complexes like cisplatin, carboplatin, and oxaliplatin are use commonly in the treatment of a multitude of cancers (149). Cisplatin has the ability to bind to DNA, inhibit DNA replication, and decrease DNA repair, making it a great candidate to use in combination with chemotherapy (150). Each of these platinum-based complexes form intrastrand DNA cross-links and DNA adducts in a cell, which ultimately leads to the induction of apoptosis of that cell (151).

Another platinum-based complex, Pt(II) 2,6-dipyrido-4-methyl-benzenechloride, was studied for its efficacy in killing cervical, colorectal, and bladder cancer cells. This complex was found to be photostable and could be activated upon irradiation with visible light (405 nm). This complex was also found to have high efficacy against the listed cell types and a cisplatin resistant bladder cell line

(EJ-R) at concentrations of 0.1-1 μM. Upon irradiation, this complex was able to kill these cancer cells through DNA single strand breakage and the generation of ROS, making it a very promising PDT agent (152).

<Figure 17>

These three compounds were tested *in vitro* against multiple cell lines in conjunction with the PS temoporofin (mTHPC), shown in Fig. 18. The synergistic effects of these compounds as PDT agents were tested against A-427 human lung cancer cells, BHY human oral cancer cells, KYSE-70 human oesophageal cancer cells, RT-4 human bladder cancer cells, and SISO human cervical cancer cells. Synergism was found when mTHPC was combined with cisplatin in KYSE-70 cells and in SISO cells. Synergism was also found when carboplatin was combined with mTHPC-PDT in SISO cells. Oxaliplatin with mTHPC was synergistic in BHY cells. Antagonistic effects were found when cisplatin was combined with mTHPC-PDT in A-427 and BHY cells. Carboplatin produced antagonistic effects when combined with mTHPC-PDT in A-427 and KYSE-70 cells. With any combination, only antagonistic effects were found in A-427 cells, and only synergistic effects were found in SISO cells. The formation of ROS with the combination therapy of mTHPC-PDT was examined. When compared to the mTHPC or Pt(II) complexes alone, there was an enhanced generation of ROS with oxaliplatin in BHY cells and RT-4 cells, and with cisplatin, carboplatin, and oxaliplatin in SISO cells (149).

<Figure 18>

Low dose carboplatin is also a good candidate for PDT against metastatic ovarian cancer. Metastatic ovarian cancer is difficult to treat due to chemoresistance and poor drug penetration, and PDT sensitizes ovarian tumours to platinum agents. The cytotoxicity of carboplatin in combination with PDT was tested *in vitro* against 3-D multicellular tumour nodules of OVCAR5 cells in order to represent the micro metastatic disease. Testing showed that treatment of these 3-D multicellular tumour nodules was dependent upon order of treatment with the carboplatin and BPD-PDT. Treating cells with BPD-PDT prior to treating with carboplatin resulted in increased synergistic reduction, while the reverse resulted in no synergism. These results indicate that PDT in combination with carboplatin is an effective treatment option to overcome resistance mechanisms and that BPD-PDT itself is also cytotoxic. The experiment with 3-D multicellular tumour nodules showed that BPD-PDT

disrupts nodular architecture of tumours, making them more vulnerable to carboplatin and nuclear apoptotic signalling (153).

PDT in combination with carboplatin and Photofrin has also been tested against HeLa cells. When HeLa cells were treated with 100 μM of carboplatin and 20 μM of Photofrin and 330 mJ of light, there was an enhanced reduction of 67.5±6.9 or 43.7±3.1% compared to Photofrin PDT alone. For PF-PDT alone, primary cell death was achieved by cell necrosis, but for ccPDT, enhanced apoptosis was observed. The generation of ROS was also observed. The low dose carboplatin-based PDT combination treatment led to the synergistic enhanced generation of toxic $^\bullet$OH *via* a Fenton-like reaction: $2[Pt^{II}]_2 + H_2O_2 \rightarrow [Pt^{2.25}]_4 + OH^- + {}^\bullet OH$. This led to superimposed apoptotic cell death without having the side effects of reducing the carboplatin dosage. This treatment will promote complete tumour regression in cervical or endometrial patients, relapse free, as a fertility-preservation therapy (154).

**GOLD**

Gold NPs have been studied for their anti-cancer properties against breast cancer (155). Au NPs were functionalized with a mixed monolayer of zinc phthalocyanine and a lactose derivative in order to study their targeting ability toward the galectin-1 receptor on the surface of breast cancer cells (156). Galectin-1 is associated with metastasis, increased tumour aggressiveness, poor prognosis, and increased cell adhesion, making it an excellent candidate for targeting (157, 158). Because lactose contains both galactose and glucose residues, and galectin-1 binds to both of these sugar units, it makes lactose the ideal candidate for targeted PDT. The study used two octa-alkyl substituted zinc(II) Pcs, with different lengths of the carbon chain connecting the macrocycle to the disulfide bond, either eleven carbon atoms (lactose-C11Pc-AuNPs), or (lactose-C3Ps-AuNPs). Both nanoparticle systems generated $^1O_2$, with lactose-C3Pc-AuNPs producing more than lactose-C11PC-AuNPs, most likely because of the enhanced surface effects on the C3Pc molecule. SK-BR-3 breast adenocarcinoma cells, MDA-MB-231 cells, and noncancerous MCF-10A cells were tested. Since it was shown that there is a higher expression of galectin-1 on the surface of the MDA-MB-231 cells, it was expected to be a better target for the lactose-C3Pc-AuNPs or lactose-C11Pc-AuNPs than the SK-BR-3 cell line. After irradiation with a 633 nm HeNe laser for 6 min, the results also showed approximately a 95% decrease in cell viability in the cancerous cell lines, and the cell viability of the lactose-containing

compound did not decrease significantly more than the compound that does not contain lactose. Lactose-C11-AuNPs targeted the SK-BR-3 cells, which lead to a significant cytotoxicity (90% at 0.2 µM) as compared to the control C11-sPED-AuNPs (61% at 0.2 µM). These results also showed that C3Pc should be used preferentially over C11Pc, because it presents higher levels of cytotoxicity for both cell lines at a lower PS concentration (157).

Au NPs in combination with PDT were tested to determine their targeting abilities toward HER2 receptors. When antibodies or cell-targeting peptides are integrated onto the nanoparticle surface it enables selective cell and/or nuclear targeting. Au NPs (4 nm) were stabilized with a self-assembled layer of a zinc–phthalocyanine derivative as a PS and a heterobifunctional polyethylene glycol. Anti-HER2 monoclonal antibodies were covalently bound to the NPs *via* a terminal carboxy moiety on the polyethylene glycol. The efficacy of phthalocyanine derivatives as a PS can be significantly enhanced by attachment to the surface of Au NPs. The C11Pc–PEG–antibody– Au NPs were tested against breast carcinoma cells MDA-MB-231 and SK-BR-3, and non-cancerous breast epithelial MCF-10A cells *in vitro*. MDA-MB-231 does not overly express HER2, and SK-BR-3 does overly express HER2. Nanoparticle conjugates can be used to specifically target and destroy HER2 cell receptor positive with PDT. Upon irradiation with 633 nm red light, SK-BR-3 exhibited a 60% decrease in cell viability, MDA-MB-231 exhibited a 25% decrease in cell viability, and MCF-10A only showed a 7% decrease in viability. The highest level of membrane damage was found in the SK-BR-3 cell line, due to the formation of, chromatin fragments. The membrane remained intact in MCF-10A cells. The 4-component nanoparticle conjugate proved to be able to specifically target and kill cancer cells through apoptosis. The results show that the 4-component nanoparticle conjugate has great potential for targeted PDT treatment of HER2+ breast cancer (156).

## LANTHANIDES

Neodymium laser treatment (Nd-YAG) has been used as a palliative care option for lung cancer patients because of its capabilities to open endobronchial stenosis and reduce obstructions since the 1980s (159). More recently, a neodymium PS complex, $NaYF_4:Yb/Er/Nd@NaYF_4:Nd$ core-shell dual PS merocyanine 540 (MC540) and ZnPc up conversion nanoparticle (UCNP) system, was synthesized to address the need for PDT agents with deeper penetrative excitability and ROS production. Specifically, Yang's laboratory sought to synthesize a novel PDT agent with laser light

excitability toward the upper limit of the PDT window of therapeutic light, in order to penetrate tissues deeper. *In vitro* and *in vivo* studies showed tumour-specific targeting ability toward folate receptor (FR)-overexpressed cancer cells. Minimal side effects were observed in normal tissue with the dual PS loaded UCNP system with folic acid (FA). PDT treatment showed the complex exhibited an enhanced PDT efficacy with the dual-PS method. Tumour cell specificity makes this PS a valuable complex for further examination (160).

Lu *et al.* reported the synthesis of a novel nanoparticle-PS conjugate capable of deep issue penetration by X-ray mediated PDT. The NP-PS $\beta$-NaLuF$_4$:X%Tb$^{3+}$ synthesis was reported (161). A terbium oxide complex, Tb$_2$O$_3$ combined with a polysiloxane layer, was synthesized and generated $^1$O$_2$ after X-ray radiation. X-ray radiation and PSs are combined here to promote a deeper therapeutic light penetration into the target tissue. Results reveal the Tb oxide complex as a possible future candidate as an anti-cancer PS due to its ability to generate $^1$O$_2$ after X-ray radiation (162).

Current studies have shown cytotoxic effects of dysprosium ion Dy$^{3+}$ upon activation by a NIR (980 nm) light treatment. Cytotoxic $^1$O$_2$ generation was detected. These nanocrystals could be useful as a penetrative NIR activated PDT agent or used in image-guided diagnosis as dark MRI contrast (163). Holmium laser fulguration, with subsequent mitomycin C installation, is a safe and feasible alternative to transurethral resection of bladder tumours (164). Holmium lasers are also utilized for the PDT treatment of Extramammary Paget's disease (EMPD), which is a rare intraepithelial neoplasm arising in apocrine rich area of the skin. A case of postoperative recurrent EMPD treated by combination therapy of non-invasive repeatable ALA-PDT and deep penetrated holmium laser was reported (165). Er:YAG laser (erbium-doped yttrium aluminium garnet laser) in combination with a topical treatment of ALA methyl ester has been proven to be effective in the photodynamic treatment of basal cell carcinoma. This treatment combination has an efficacy of 98.97% against basal cell carcinoma. The preferred treatment method was the Er:YAG laser, with an efficacy of 91.75% (166).

The Ytterbium ion Yb$^{3+}$ has been tested upon irradiation to determine the efficacy of PDT upon excitation to its triplet state (167). Ytterbium-doped fibre laser can be one of the simplest methods for the creation of the high-power sources for the excitation of $^1$O$_2$. A study reported a drug-free form of PDT using an ytterbium-doped fibre laser, an SRS converter, and a maximum output

power of 18 W at a wavelength of 0.97 μm in the treatment of basalioma. The preliminary results showed a relatively high efficiency of the device in the organ preserving treatment of basaliomas, even in the case of inconvenient localizations with good cosmetic results (168).

A $Y_{2.99}Pr_{0.01}Al_5O_{12}$-based (YP) mesoporous silica coated nanoparticle, with protoporphyrin IX (PpIX) and folic acid (YPMS@PpIX@FA), was reported to address the need for X-ray mediated PDT agents with potentially deeper tissue penetrative abilities. Other researchers have developed PSs with the same goals and have shown X-ray mediated PDT can penetrate tissue deeper than the typical visible light induced PDT, which reduces the limitations in treatment application of PDT (169). *In vitro* studies in breast and prostate cancer cells showed YPMS@PpIX@FA nanocomposites were integrated into cancer cells with the folate receptor Folr1. *In vivo* studies showed good biocompatibility (170). Folr1 is often chosen to target cancer cells with treatments because tumour cells often overexpress the receptor (171). Therefore, utilization of this tumour selectivity method specifies the therapeutic agent's role. Good biocompatibility is an ideal pharmacokinetic property in drug delivery, making this PS an interesting candidate for future studies (75).

Lu *et al.* reported the synthesis of a novel nano particle-PS conjugate capable of deep tissue penetration by X-ray mediated PDT. The NP-PS $\beta$-NaLuF$_4$: X%Tb$^{3+}$ synthesis was reported (161). A Tb oxide complex, $Tb_2O_3$ combined with a polysiloxane layer, was synthesized and generated $^1O_2$ after X-ray radiation. X-ray radiation and PSs are combined here to promote a deeper therapeutic light penetration into the target tissue. Results reveal the Tb oxide complex as a possible future candidate as an anti-cancer PS due to its ability to generate $^1O_2$ after X-ray radiation (162)

The Ytterbium ion Yb$^{3+}$ has been tested upon irradiation to determine the efficacy of PDT upon excitation to its triplet state (167). Ytterbium-doped fibre laser can be one of the simplest methods for the creation of the high-power sources for the excitation of $^1O_2$. A study reported a drug-free form of PDT using an ytterbium-doped fibre laser, an SRS converter, and a maximum output power of 18 W at a wavelength of 0.97 μm in the treatment of basalioma. The preliminary results showed a relatively high efficiency of the device in the organ preserving treatment of basaliomas, even in the case of inconvenient localizations with good cosmetic results (168).

Pre-clinical, *in vivo* studies of motexafin lutetium for the PDT treatment of rectal cancer in dogs has been observed (172). The dosage for the PDT treatment was 2 mg kg$^{-1}$ of motexafin lutetium with pelvic illumination of the transected distal rectum with 730 nm of light, with doses ranging from 0.5 to 10 J cm$^{-2}$ 3 hours post drug delivery. Results showed no severe toxicity or anastomotic leak, and low photobleaching. Drug uptake levels in the colon of photosensitized dogs were much higher than that of the controls or of the dogs that did not undergo PDT. Drug uptake in the rectum was found to be $0.72 \pm 0.23$ ng mg$^{-1}$. Motexafin lutetium mediated PDT with 730 nm of light is an adequate treatment for the residual microscopic cancer at less than 5 mm of depth. Overall, motexafin lutetium mediated PDT is an effective adjunctive therapy for the treatment of rectal cancer and will possibly evaluated further in clinical trials (172).

## CLINICAL TRIALS INVOLVING PDT AND COMPLEXES

TLD1433 is the most prominent and newly developed ruthenium-based photosensitizer that has passed phase I clinical trial for the treatment of non-muscle invasive bladder cancer. TLD1433 has been proven to have a greater phototoxicity than Photofrin for the PDT treatment of this cancer and is effectively cell selective (173).

A clinical trial assessing the safety and response to PDT with a Tookad PS was performed in patients with recurrent prostate cancer. After PDT with Tookad, MRIs showed lesion formation was strongly drug and light dose dependent (174). These results revealed the cytotoxic abilities of Pd complexes in PDT, outlining new applications for Pd-containing species.

Mang *et al.* investigated a PDT palliative option for breast cancer patients with recurring breast cancer in a phase II/III clinical trial. Patients were treated with Purlytin. Six months follow up showed a 92% PDT response rate, and 8% partial response (175). Purlytin had a 100% response rate among the patients within this trial, and no adverse effects as a result of the treatment. This is an especially important development for successful PDT palliative care options.

The drug motexafin lutetium (lutetium texaphyrin, Optrin, Lu-Tex), marketed as Antrin by Pharamacyclics Inc., has shown promising results in the PDT treatment of many diseases and cancers. Patients with locally recurrent prostate carcinoma, after receiving radiation treatment, were selected for motexafin lutetium mediated PDT in a phase I clinical trial (176-179). Patients in this clinical trial were administered with motexafin lutetium through IV at 0.5 to 2 mg kg$^{-1}$ 24, 6, or 3 hours prior to

PDT treatment with 732 nm light delivery with a fluence rate of 150 mW cm$^{-1}$ and a light fluence rate of 25 to 150 J cm$^{-2}$. Optic fibers were utilized for light delivery and delivered through a transperineal brachytherapy template. Patients showed large, transient increases in serum PSA (prostate-specific antigen) after PDT treatment. After 26 to 55 days, the PSA levels dropped to an indistinguishable level from the baseline. It was determined that all patients presented a significant uptake of this PS in the prostate. Adverse effects form this specific protocol such as photobleaching, tissue damage, and a drastic increase in PSA levels should bring caution that such PDT treatment using motexafin lutetium requires a more individualized treatment for each patient (176-179). Motexafin lutetium has been examined in a phase I clinical trial for the treatment of cervical intraepithelial neoplasia grade 2 and 3 (180), and in a phase II clinical trial for the treatment of recurrent breast cancer (181).

<Table 1>

**CONCLUSION**

To conclude, PDT has been proven in many studies to be an effective treatment for multiple types of cancers. PDT uses a PS that, upon irradiation with light, produces ROS, or hydroxyl radicals through a Fenton reaction. The generation of these ROS have been proven to kill cancer cells, and in many cases, through induced apoptosis. This review discussed many metal-based compounds, as well as compounds with lanthanides used in *in vitro*, *in vivo* studies, as well as clinical trials. These complexes act as efficacious photosensitizers and are cytotoxic to cancer cells both upon irradiation with light, and in some cases, cytotoxic by themselves. PDT can be used as a powerful form of cancer treatment that can be localized, as it has been proven to be successful in specifically targeting cancer cells without harming normal healthy cells.

**References**

1.  Siegel, R. L., K. D. Miller, A. Goding Sauer, S. A. Fedewa, L. F. Butterly, J. C. Anderson, A. Cercek, R. A. Smith and A. Jemal (2020) Colorectal cancer statistics, 2020. *CA Cancer J. Clin.*

2.  Henley, S. J., C. C. Thomas, D. R. Lewis, E. M. Ward, F. Islami, M. Wu, H. K. Weir, S. Scott, R. L. Sherman and J. Ma (2020) Annual report to the nation on the status of cancer, part II: Progress toward Healthy People 2020 objectives for 4 common cancers. *Cancer* **126,** 2250-2266.

3.  Kohler, B. A., R. L. Sherman, N. Howlader, A. Jemal, A. B. Ryerson, K. A. Henry, F. P. Boscoe, K. A. Cronin, A. Lake and A.-M. Noone (2015) Annual report to the nation on the status of cancer, 1975-2011, featuring incidence of breast cancer subtypes by race/ethnicity, poverty, and state. *J. Natl. Cancer Inst.* **107**.

4.  Bray, F., J. Ferlay, I. Soerjomataram, R. L. Siegel, L. A. Torre and A. Jemal (2018) Global cancer statistics 2018: GLOBOCAN estimates of incidence and mortality worldwide for 36 cancers in 185 countries. *CA Cancer J. Clin.* **68,** 394-424.

5.  Ward, E. M., R. L. Sherman, S. J. Henley, A. Jemal, D. A. Siegel, E. J. Feuer, A. U. Firth, B. A. Kohler, S. Scott and J. Ma (2019) Annual report to the nation on the status of cancer, featuring cancer in men and women age 20–49 years. *J. Natl. Cancer Inst.* **111,** 1279-1297.

6.  Jemal, A., R. Siegel, J. Xu and E. Ward (2010) Cancer statistics, 2010. *CA Cancer J. Clin.* **60,** 277-300.

7.  Gores, G. J. and D. Lieberman (2016) Good news–bad news: current status of GI cancers. *Gastroenterology* **151,** 13-16.

8.  Underwood, J. M., T. B. Richards, S. J. Henley, B. Momin, K. Houston, I. Rolle, C. Holmes and S. L. Stewart (2015) Decreasing trend in tobacco-related cancer incidence, United States 2005–2009. *J. Commun. Health* **40,** 414-418.

9.  Dite, G. S., M. Mahmoodi, A. Bickerstaffe, F. Hammet, R. J. Macinnis, H. Tsimiklis, J. G. Dowty, C. Apicella, K.-A. Phillips and G. G. Giles (2013) Using SNP genotypes to improve the discrimination of a simple breast cancer risk prediction model. *Breast Cancer Res. Treat.* **139,** 887-896.

10.    Gradishar, W. J., D. Krasnojon, S. Cheporov, A. N. Makhson, G. M. Manikhas, A. Clawson, P. Bhar, J. R. McGuire and J. Iglesias (2012) Phase II trial of nab-paclitaxel compared with docetaxel as first-line chemotherapy in patients with metastatic breast cancer: final analysis of overall survival. *Clin. Breast Cancer* **12,** 313-321.

11.    Mao, J., Y. Zhang, J. Zhu, C. Zhang and Z. Guo (2009) Molecular combo of photodynamic therapeutic agent silicon (IV) phthalocyanine and anticancer drug cisplatin. *Chem. Commun.***,** 908-910.

12.    Lovell, J. F., T. W. Liu, J. Chen and G. Zheng (2010) Activatable photosensitizers for imaging and therapy. *Chem. Rev.* **110,** 2839-2857.

13.    Raab, O. (1900) Uber die wirkung fluorescirender stoffe auf infusorien. *Z. Biol.* **39,** 524-546.

14.    Von Tappeiner, H. (1900) Uber die Wirkung fluoreszierender Stoffe auf Infusorien nach Versuchen von O. Raab. *Muench. Med. Wochenschr.* **47**.

15.    Von Tappeiner, H. (1903) Therapeutische versuche mit fluoreszierenden stoffen. *Munch. Med. Wochenschr.* **1,** 2042-2044.

16.    Corti, L., L. Toniolo, C. Boso, F. Colaut, D. Fiore, P. C. Muzzio, M. I. Koukourakis, R. Mazzarotto, M. Pignataro and L. Loreggian (2007) Long-term survival of patients treated with photodynamic therapy for carcinoma in situ and early non-small-cell lung carcinoma. *Lasers Surg. Med.* **39,** 394-402.

17.    Nowis, D., M. Makowski, T. Stokłosa, M. Legat, T. Issat and J. Gołab (2005) Direct tumor damage mechanisms of photodynamic therapy. *Acta Biochim. Pol.* **52,** 339-352.

18.    Boodram, S., J. L Bullock, V. H Rambaran and A. A Holder (2017) The use of inorganic compounds in photodynamic therapy: improvements in methods and photosensitizer design. *Recent Pat. Nanotechnol.* **11,** 3-14.

19.    Ochsner, M. (1997) Photophysical and photobiological processes in the photodynamic therapy of tumours. *J. Photochem. Photobiol., B* **39,** 1-18.

20.    Mackay, F. S., J. A. Woods, P. Heringová, J. Kašpárková, A. M. Pizarro, S. A. Moggach, S. Parsons, V. Brabec and P. J. Sadler (2007) A potent cytotoxic photoactivated platinum complex. *Proc. Natl. Acad. Sci.* **104,** 20743-20748.

21. Lucky, S. S., K. C. Soo and Y. Zhang (2015) Nanoparticles in photodynamic therapy. *Chem. Rev.* **115,** 1990-2042.

22. Szaciłowski, K., W. Macyk, A. Drzewiecka-Matuszek, M. Brindell and G. Stochel (2005) Bioinorganic photochemistry: frontiers and mechanisms. *Chem. Rev.* **105,** 2647-2694.

23. Bonnett, R. (1995) Photosensitizers of the porphyrin and phthalocyanine series for photodynamic therapy. *Chem. Soc. Rev.* **24,** 19-33.

24. Dolmans, D. E., D. Fukumura and R. K. Jain (2003) Photodynamic therapy for cancer. *Nat. Rev. Cancer* **3,** 380-387.

25. DeRosa, M. C. and R. J. Crutchley (2002) Photosensitized singlet oxygen and its applications. *Coord. Chem. Rev.* **233,** 351-371.

26. Schweitzer, V. G. (2001) PHOTOFRIN-mediated photodynamic therapy for treatment of early stage oral cavity and laryngeal malignancies. *Lasers Surg. Med.* **29,** 305-313.

27. Ackroyd, R., C. Kelty, N. Brown and M. Reed (2001) The history of photodetection and photodynamic therapy¶. *Photochem. Photobiol.* **74,** 656-669.

28. Devi, J., M. Yadav, D. Jindal, D. Kumar and Y. Poornachandra (2019) Synthesis, spectroscopic characterization, biological screening and in vitro cytotoxic studies of 4-methyl-3-thiosemicarbazone derived Schiff bases and their Co (II), Ni (II), Cu (II) and Zn (II) complexes. *Appl. Organomet. Chem.* **33,** e5154.

29. Bonnett, R. (2000) *Chemical aspects of photodynamic therapy.* CRC Press, London, UK.

30. Akaza, E., M. Yuzawa, Y. Matsumoto, S. Kashiwakura, K. Fujita and R. Mori (2007) Role of photodynamic therapy in polypoidal choroidal vasculopathy. *Jpn. J. Ophthalmol.* **51,** 270-277.

31. McKenzie, L. K., H. E. Bryant and J. A. Weinstein (2019) Transition metal complexes as photosensitisers in one-and two-photon photodynamic therapy. *Coord. Chem. Rev.* **379,** 2-29.

32. Felder, P. S., S. Keller and G. Gasser (2020) Polymetallic Complexes for Applications as Photosensitisers in Anticancer Photodynamic Therapy. *Adv. Ther.* **3,** 1900139.

33. Mari, C., V. Pierroz, S. Ferrari and G. Gasser (2015) Combination of Ru (II) complexes and light: new frontiers in cancer therapy. *Chem. Sci.* **6,** 2660-2686.

34. Garai, A., I. Pant, P. Kondaiah and A. R. Chakravarty (2015) Iron (III) salicylates of dipicolylamine bases showing photo-induced anticancer activity and cytosolic localization. *Polyhedron* **102,** 668-676.

35. Stacey, O. J. and S. J. Pope (2013) New avenues in the design and potential application of metal complexes for photodynamic therapy. *RSC Adv.* **3,** 25550-25564.

36. Knoll, J. D. and C. Turro (2015) Control and utilization of ruthenium and rhodium metal complex excited states for photoactivated cancer therapy. *Coord. Chem. Rev.* **282,** 110-126.

37. Yano, T., S. Hishida, M. Nakai and Y. Nakabayashi (2017) Anticancer activity of heterodinuclear ruthenium (II)–platinum (II) complexes as photochemotherapeutic agents. *Inorg. Chim. Acta* **454,** 162-170.

38. Mahata, S., S. Mukherjee, S. K. Tarai, A. Pan, I. Mitra, S. Pal, S. Maitra and S. C. Moi (2019) Synthesis and characterization of Pt (ii)-based potent anticancer agents with minimum normal cell toxicity: their bio-activity and DNA-binding properties. *New J. Chem.* **43,** 18767-18779.

39. Robertson, C. A., D. H. Evans and H. Abrahamse (2009) Photodynamic therapy (PDT): a short review on cellular mechanisms and cancer research applications for PDT. *J. Photochem. Photobiol., B* **96,** 1-8.

40. Lilge, L. (2018) Use of Ruthenium Complexes as Photosensitizers in Photodynamic Therapy. In *Ruthenium Complexes*. (Edited by A. A. H. W. R. Browne, M. A. Lawrence, J. L. Bullock Jr, L. Lilge), pp. 117-137. Wiley-VCH Verlag GmbH & Co. KGaA, Weinheim Germany.

41. Bullock, J. L. and A. A. Holder (2018) Photodynamic Therapy in Medicine with Mixed-Metal/Supramolecular Complexes. In *Ruthenium Complexes*. (Edited by A. A. H. W. R. Browne, M. A. Lawrence, J. L. Bullock Jr, L. Lilge), pp. 139-160. Wiley-VCH Verlag GmbH & Co. KGaA, Weinheim Germany.

42. Beer, M. D. and S. Swavey (2018) Design Aspects of Ruthenium Complexes as DNA Probes and Therapeutic Agents. In *Ruthenium Complexes*. (Edited by A. A. H. W. R. Browne, M. A. Lawrence, J. L. Bullock Jr, L. Lilge), pp. 181-200. Wiley-VCH Verlag GmbH & Co. KGaA, Weinheim Germany

43. Kyriazi, M., E. Alexandratou, D. Yova, M. Rallis and T. Trebst (2008) Topical photodynamic therapy of murine non-melanoma skin carcinomas with aluminum phthalocyanine chloride

and a diode laser: pharmacokinetics, tumor response and cosmetic outcomes. *Photodermatol. Photoimmunol. Photomed.* **24,** 87-94.

44.  Maduray, K., B. Odhav and T. Nyokong (2012) In vitro photodynamic effect of aluminum tetrasulfophthalocyanines on melanoma skin cancer and healthy normal skin cells. *Photodiagn. Photodyn. Ther.* **9,** 32-39.

45.  Hopper, C. (2000) Photodynamic therapy: a clinical reality in the treatment of cancer. *Lancet Oncol.* **1,** 212-219.

46.  Castano, A. P., T. N. Demidova and M. R. Hamblin (2004) Mechanisms in photodynamic therapy: part one—photosensitizers, photochemistry and cellular localization. *Photodiagn. Photodyn. Ther.* **1,** 279-293.

47.  Detty, M. R., S. L. Gibson and S. J. Wagner (2004) Current clinical and preclinical photosensitizers for use in photodynamic therapy. *J. Med. Chem.* **47,** 3897-3915.

48.  Sutoris, K., J. Rakusan, M. Karaskova, J. Mattova, J. Benes, M. Nekvasil, P. Jezek, M. Zadinova, P. Pouckova and D. Vetvicka (2013) Novel topical photodynamic therapy of prostate carcinoma using hydroxy-aluminum phthalocyanine entrapped in liposomes. *Anticancer Res.* **33,** 1563-1568.

49.  Yang, C.-C., Y.-J. Sun, P.-H. Chung, W.-Y. Chen, W. Swieszkowski, W. Tian and F.-H. Lin (2017) Development of Ce-doped TiO2 activated by X-ray irradiation for alternative cancer treatment. *Ceram. Int.* **43,** 12675-12683.

50.  Yang, C.-C., M.-H. Tsai, K.-Y. Li, C.-H. Hou and F.-H. Lin (2019) Carbon-doped TiO2 activated by X-ray irradiation for the generation of reactive oxygen species to enhance photodynamic therapy in tumor treatment. *Int. J. Mol. Sci.* **20,** 2072.

51.  Crans, D. C., L. Henry, G. Cardiff and B. I. Posner (2019) Developing vanadium as an antidiabetic or anticancer drug: a clinical and historical perspective. *Met. Ions Life Sci.*, 203-230.

52.  Sasmal, P. K., A. K. Patra, M. Nethaji and A. R. Chakravarty (2007) DNA cleavage by new oxovanadium (IV) complexes of N-salicylidene α-amino acids and phenanthroline bases in the photodynamic therapy window. *Inorg. Chem.* **46,** 11112-11121.

53. Kumar, A., A. Dixit, S. Sahoo, S. Banerjee, A. Bhattacharyya, A. Garai, A. A. Karande and A. R. Chakravarty (2020) Crystal structure, DNA crosslinking and photo-induced cytotoxicity of oxovanadium (IV) conjugates of boron-dipyrromethene. *J. Inorg. Biochem.* **202,** 110817.

54. Banik, B., K. Somyajit, G. Nagaraju and A. R. Chakravarty (2014) Oxovanadium (IV) catecholates of terpyridine bases for cellular imaging and photocytotoxicity in red light. *RSC Adv.* **4,** 40120-40131.

55. Das, S., J. M. Dowding, K. E. Klump, J. F. McGinnis, W. Self and S. Seal (2013) Cerium oxide nanoparticles: applications and prospects in nanomedicine. *Nanomedicine* **8,** 1483-1508.

56. Atif, M., S. Iqbal, M. Ismail, Q. Mansoor, L. Mughal, M. H. Aziz, A. Hanif and W. Farooq (2019) Manganese-doped cerium oxide nanocomposite induced photodynamic therapy in MCF-7 cancer cells and antibacterial activity. *Biomed. Res. Int.* **2019**.

57. Chen, Q., Y. Ma, P. Bai, Q. Li, B. S. Canup, D. Long, B. Ke, F. Dai, B. Xiao and C. Li (2021) Tumor Microenvironment-Responsive Nanococktails for Synergistic Enhancement of Cancer Treatment via Cascade Reactions. *ACS Appl. Mater. Interfaces*.

58. Liu, Y., J. Yang, B. Liu, W. Cao, J. Zhang, Y. Yang, L. Ma, J. M. de la Fuente, J. Song and J. Ni (2020) Human iPS Cells Loaded with MnO 2-Based Nanoprobes for Photodynamic and Simultaneous Enhanced Immunotherapy Against Cancer. *Nano-Micro Lett.* **12,** 1-17.

59. Tabrizi, L. (2018) Novel cyclometalated Fe (II) complex with NCN pincer and BODIPY-appended 4'-ethynyl-2, 2': 6', 2''-terpyridine as mitochondria-targeted photodynamic anticancer agents. *Appl. Organomet. Chem.* **32,** e4161.

60. Sun, Y.-M., W. Akram, F. Cheng, Z.-Y. Liu, Y.-H. Liao, Y. Ye and H.-Y. Liu (2019) DNA interaction and photodynamic antitumor activity of transition metal mono-hydroxyl corrole. *Bioorg. Chem.* **90,** 103085.

61. Heffern, M. C., N. Yamamoto, R. J. Holbrook, A. L. Eckermann and T. J. Meade (2013) Cobalt derivatives as promising therapeutic agents. *Curr. Opin. Chem. Biol.* **17,** 189-196.

62. Thakur, Y., R. Agrawal, M. Tripathi, M. K. Siddiqi, E. Mohapatra, R. H. Khan and R. Pande (2019) Exploring the DNA binding efficacy of Cobalt (II) and Copper (II) complexes of hydroxamic acids and explicating their anti-cancer propensity. *J. Mol. Struct.* **1197,** 691-706.

63. Renfrew, A. K., N. S. Bryce and T. Hambley (2015) Cobalt (III) Chaperone Complexes of Curcumin: Photoreduction, Cellular Accumulation and Light-Selective Toxicity towards Tumour Cells. *Chem. Eur. J.* **21,** 15224-15234.

64. Das, D., A. Banaspati, N. Das, B. Bora, M. K. Raza and T. K. Goswami (2019) Visible light-induced cytotoxicity studies on Co (ii) complexes having an anthracene-based curcuminoid ligand. *Dalton Trans.* **48,** 12933-12942.

65. Roy, S., S. Roy, S. Saha, R. Majumdar, R. R. Dighe, E. D. Jemmis and A. R. Chakravarty (2011) Cobalt (II) complexes of terpyridine bases as photochemotherapeutic agents showing cellular uptake and photocytotoxicity in visible light. *Dalton Trans.* **40,** 1233-1242.

66. Moosa, B., K. Fhayli, S. Li, K. Julfakyan, A. Ezzeddine and N. M. Khashab (2014) Applications of nanodiamonds in drug delivery and catalysis. *J. Nanosci. Nanotechnol.* **14,** 332-343.

67. Sivakumar, B., R. G. Aswathy, R. Sreejith, Y. Nagaoka, S. Iwai, M. Suzuki, T. Fukuda, T. Hasumura, Y. Yoshida and T. Maekawa (2014) Bacterial exopolysaccharide based magnetic nanoparticles: a versatile nanotool for cancer cell imaging, targeted drug delivery and synergistic effect of drug and hyperthermia mediated cancer therapy. *J. Biomed. Nanotechnol.* **10,** 885-899.

68. Yuan, M., S. Xu, Q. Zhang, B. Zhao, B. Feng, K. Ji, L. Yu, W. Chen, M. Hou, Y. Xu and X. Fu (2020) Bicompatible porous Co3O4 nanoplates with intrinsic tumor metastasis inhibition for multimodal imaging and DNA damage–mediated tumor synergetic photothermal/photodynamic therapy. *Chem. Eng. J.* **394**.

69. Park, B. J., K.-H. Choi, K. C. Nam, A. Ali, J. E. Min, H. Son, H. S. Uhm, H.-J. Kim, J.-S. Jung and E. H. Choi (2015) Photodynamic anticancer activities of multifunctional cobalt ferrite nanoparticles in various cancer cells. *J. Biomed. Nanotechnol.* **11,** 226-235.

70. Choi, K.-H., K. C. Nam, U.-H. Kim, G. Cho, J.-S. Jung and B. J. Park (2017) Optimized photodynamic therapy with multifunctional cobalt magnetic nanoparticles. *Nanomaterials* **7,** 144.

71. Zamble, D. (2017) Introduction to the Biological Chemistry of Nickel.

72.    Kumar, S. and A. Trivedi (2016) A review on role of nickel in the biological system. *Int. J. Curr. Microbiol. App. Sci* **5,** 719-727.

73.    Sweigert, P., Z. Xu, Y. Hong and S. Swavey (2012) Nickel, copper, and zinc centered ruthenium-substituted porphyrins: effect of transition metals on photoinduced DNA cleavage and photoinduced melanoma cell toxicity. *Dalton Trans.* **41,** 5201-5208.

74.    Er, O., F. Y. Lambrecht, K. Ocakoglu, C. Kayabasi and C. Gunduz (2015) Primary evaluation of a nickel-chlorophyll derivative as a multimodality agent for tumor imaging and photodynamic therapy. *J. Radioanal. Nucl. Chem.* **306,** 155-163.

75.    Hamblin, M. R. (2018) Photodynamic Therapy and Photobiomodulation: Can All Diseases be Treated with Light? **,** pp. 100-135.

76.    Mukherjee, N., S. Podder, S. Banerjee, S. Majumdar, D. Nandi and A. R. Chakravarty (2016) Targeted photocytotoxicity by copper (II) complexes having vitamin B6 and photoactive acridine moieties. *Eur. J. Med. Chem.* **122,** 497-509.

77.    Lin, R. K., C. I. Chiu, C. H. Hsu, Y. J. Lai, P. Venkatesan, P. H. Huang, P. S. Lai and C. C. Lin (2018) Photocytotoxic Copper (II) Complexes with Schiff-Base Scaffolds for Photodynamic Therapy. *Chem. Eur. J.* **24,** 4111-4120.

78.    Musib, D., M. K. Raza, S. Kundu and M. Roy (2018) Modulating In Vitro Photodynamic Activities of Copper (II) Complexes. *Eur. J. Inorg. Chem.* **2018,** 2011-2018.

79.    Ruan, Y., X. Jia, C. Wang, W. Zhen and X. Jiang (2019) Methylene Blue Loaded Cu–Tryptone Complex Nanoparticles: A New Glutathione-Reduced Enhanced Photodynamic Therapy Nanoplatform. *ACS Biomater. Sci. Eng.* **5,** 1016-1022.

80.    Rodal, G. H., S. K. Rodal, J. Moan and K. Berg (1998) Liposome-bound Zn (II)-phthalocyanine. Mechanisms for cellular uptake and photosensitization. *J. Photochem. Photobiol., B* **45,** 150-159.

81.    Nene, L. C., M. Managa and T. Nyokong (2019) Photo-physicochemical properties and in vitro photodynamic therapy activity of morpholine-substituted Zinc (II)-Phthalocyanines π-π stacked on biotinylated graphene quantum dots. *Dyes Pigm.* **165,** 488-498.

82.    Kee, H. L., J. Bhaumik, J. R. Diers, P. Mroz, M. R. Hamblin, D. F. Bocian, J. S. Lindsey and D. Holten (2008) Photophysical characterization of imidazolium-substituted Pd (II), In (III),

and Zn (II) porphyrins as photosensitizers for photodynamic therapy. *J. Photochem. Photobiol., A* **200,** 346-355.

83.    Pan, D., X. Zhong, W. Zhao, Z. Yu, Z. Yang, D. Wang, H. Cao and W. He (2018) Meso-substituted porphyrin photosensitizers with enhanced near-infrared absorption: synthesis, characterization and biological evaluation for photodynamic therapy. *Tetrahedron* **74,** 2677-2683.

84.    Yu, Q., W.-X. Xu, Y.-H. Yao, Z.-Q. Zhang, S. Sun and J. Li (2015) Synthesis and photodynamic activities of a new metronidazole-appended porphyrin and its Zn (II) complex. *J. Porphyrins Phthalocyanines* **19,** 1107-1113.

85.    Kirakci, K., J. Zelenka, M. Rumlová, J. Martinčík, M. Nikl, T. Ruml and K. Lang (2018) Octahedral molybdenum clusters as radiosensitizers for X-ray induced photodynamic therapy. *J. Mater. Chem.* **6,** 4301-4307.

86.    Brandhonneur, N., T. Hatahet, M. Amela-Cortes, Y. Molard, S. Cordier and G. Dollo (2018) Molybdenum cluster loaded PLGA nanoparticles: An innovative theranostic approach for the treatment of ovarian cancer *Eur. Opean J. Pharm. Biopharm.* **125,** 95-105.

87.    Frei, A., R. Rubbiani, S. Tubafard, O. Blacque, P. Anstaett, A. Felgenträger, T. Maisch, L. Spiccia and G. Gasser (2014) Synthesis, characterization, and biological evaluation of new Ru (II) polypyridyl photosensitizers for photodynamic therapy. *J. Med. Chem.* **57,** 7280-7292.

88.    Dougherty, T. J., C. J. Gomer, B. W. Henderson, G. Jori, D. Kessel, M. Korbelik, J. Moan and Q. Peng (1998) Photodynamic therapy. *J. Natl. Cancer Inst.* **90,** 889-905.

89.    Juris, A., V. Balzani, F. Barigelletti, S. Campagna, P. l. Belser and A. v. von Zelewsky (1988) Ru (II) polypyridine complexes: photophysics, photochemistry, eletrochemistry, and chemiluminescence. *Coord. Chem. Rev.* **84,** 85-277.

90.    Castano, A. P., T. N. Demidova and M. R. Hamblin (2005) Mechanisms in photodynamic therapy: part two—cellular signaling, cell metabolism and modes of cell death. *Photodiagn. Photodyn. Ther.* **2,** 1-23.

91.    Swavey, S. and K. J. Brewer (2002) Visible Light Induced Photocleavage of DNA by a Mixed-Metal Supramolecular Complex: $[\{(bpy)_2Ru(dpp)\}_2RhCl2]^{5+}$. *Inorg. Chem.* **41,** 6196-6198.

92. Zhang, P., L. Pei, Y. Chen, W. Xu, Q. Lin, J. Wang, J. Wu, Y. Shen, L. Ji and H. Chao (2013) A Dinuclear Ruthenium (II) Complex as a One-and Two-Photon Luminescent Probe for Biological Cu2+ Detection. *Chem. Eur. J.* **19,** 15494-15503.

93. Zhao, X., M. Li, W. Sun, J. Fan, J. Du and X. Peng (2018) An estrogen receptor targeted ruthenium complex as a two-photon photodynamic therapy agent for breast cancer cells. *Chem. Commun.* **54,** 7038-7041.

94. Holder, A. A., P. Taylor, A. R. Magnusen, E. T. Moffett, K. Meyer, Y. Hong, S. E. Ramsdale, M. Gordon, J. Stubbs, L. A. Seymour, D. Acharya, R. T. Weber, P. F. Smith, G. C. Dismukes, P. Ji, L. Menocal, F. Bai, J. L. Williams, D. M. Cropek and W. L. Jarrett (2013) Preliminary anti-cancer photodynamic therapeutic in vitro studies with mixed-metal binuclear ruthenium(II)-vanadium(IV) complexes. *Dalton Trans* **42,** 11881-11899.

95. Holder, A. A., S. Swavey and K. J. Brewer (2004) Design aspects for the development of mixed-metal supramolecular complexes capable of visible light induced photocleavage of DNA. *Inorg. Chem.* **43,** 303-308.

96. Holder, A. A., D. F. Zigler, M. T. Tarrago-Trani, B. Storrie and K. J. Brewer (2007) Photobiological Impact of [{(bpy) 2Ru (dpp)} 2RhCl2] Cl5 and [{(bpy) 2Os (dpp)} 2RhCl2] Cl5 [bpy= 2, 2 '-Bipyridine; dpp= 2, 3-Bis (2-pyridyl) pyrazine] on Vero Cells. *Inorg. Chem.* **46,** 4760-4762.

97. Fang, Z., S. Swavey, A. Holder, B. Winkel and K. J. Brewer (2002) DNA binding of mixed-metal supramolecular Ru, Pt complexes. *Inorg. Chem. Commun.* **5,** 1078-1081.

98. Swavey, S. and K. J. Brewer (2002) Visible light induced photocleavage of DNA by a mixed-metal supramolecular complex:[{(bpy) 2Ru (dpp)} 2RhCl2] 5+. *Inorg. Chem.* **41,** 6196-6198.

99. Hergueta-Bravo, A., M. E. Jiménez-Hernández, F. Montero, E. Oliveros and G. Orellana (2002) Singlet oxygen-mediated DNA photocleavage with Ru (II) polypyridyl complexes. *J. Phys. Chem. B* **106,** 4010-4017.

100. Monro, S., K. L. Colón, H. Yin, J. Roque III, P. Konda, S. Gujar, R. P. Thummel, L. Lilge, C. G. Cameron and S. A. McFarland (2018) Transition metal complexes and photodynamic therapy from a tumor-centered approach: Challenges, opportunities, and highlights from the development of TLD1433. *Chem. Rev.* **119,** 797-828.

101. Zhu, J., A. Dominijanni, J. Á. Rodríguez-Corrales, R. Prussin, Z. Zhao, T. Li, J. L. Robertson and K. J. Brewer (2017) Visible light-induced cytotoxicity of Ru, Os–polyazine complexes towards rat malignant glioma. *Inorg. Chim. Acta* **454,** 155-161.

102. Zhang, P., H. Huang, J. Huang, H. Chen, J. Wang, K. Qiu, D. Zhao, L. Ji and H. Chao (2015) Noncovalent ruthenium (II) complexes–single-walled carbon nanotube composites for bimodal photothermal and photodynamic therapy with near-infrared irradiation. *ACS Appl. Mater. Interfaces* **7,** 23278-23290.

103. Abbas, Z. and S. Rehman (2018) An Overview of Cancer Treatment Modalities. In *Neoplasm*. INTECHOPEN LIMITED London.

104. Paul, S., P. Kundu, U. Bhattacharyya, A. Garai, R. C. Maji, P. Kondaiah and A. R. Chakravarty (2019) Ruthenium (II) Conjugates of Boron-Dipyrromethene and Biotin for Targeted Photodynamic Therapy in Red Light. *Inorg. Chem.* **59,** 913-924.

105. Alberto, M. E., J. Pirillo, N. Russo and C. Adamo (2016) Theoretical exploration of type I/Type II dual photoreactivity of promising Ru (II) dyads for PDT approach. *Inorg. Chem.* **55,** 11185-11192.

106. Chamberlain, S., H. D. Cole, J. Roque, D. Bellnier, S. A. McFarland and G. Shafirstein (2020) TLD1433-Mediated photodynamic therapy with an optical surface applicator in the treatment of lung cancer cells in vitro. *Pharmaceuticals* **13,** 137.

107. Chen, Q., V. Ramu, Y. Aydar, A. Groenewoud, X.-Q. Zhou, M. J. Jager, H. Cole, C. G. Cameron, S. A. McFarland and S. Bonnet (2020) TLD1433 Photosensitizer inhibits conjunctival melanoma cells in zebrafish ectopic and orthotopic tumour models. *Cancers* **12,** 587.

108. Lilge, L., M. Roufaiel, S. Lazic, P. Kaspler, M. A. Munegowda, M. Nitz, J. Bassan and A. Mandel (2020) Evaluation of a Ruthenium coordination complex as photosensitizer for PDT of bladder cancer: Cellular response, tissue selectivity and in vivo response. *TBIO* **2,** e201900032.

109. Katsaros, N. and A. Anagnostopoulou (2002) Rhodium and its compounds as potential agents in cancer treatment. *Crit. Rev. Oncol. Hematol.* **42,** 297-308.

110. Kang, S., W. Shin, M.-H. Choi, M. Ahn, Y.-K. Kim, S. Kim, D.-H. Min and H. Jang (2018) Morphology-controlled synthesis of rhodium nanoparticles for cancer phototherapy. *ACS Nano* **12,** 6997-7008.

111. Machuca, A., E. Garcia-Calvo, D. S. Anunciação and J. L. Luque-Garcia (2020) Rhodium Nanoparticles as a Novel Photosensitizing Agent in Photodynamic Therapy against Cancer. *Chem. Eur. J.*

112. Ding, M., Z. Miao, F. Zhang, J. Liu, X. Shuai, Z. Zha and Z. Cao (2020) Catalytic rhodium (Rh)-based (mesoporous polydopamine) MPDA nanoparticles with enhanced phototherapeutic efficiency for overcoming tumor hypoxia. *Biomater. Sci.* **8,** 4157-4165.

113. Helmers, E. (2006) Palladium emissions in the environment analytical methods, environmental assessment and health effects. *Environ. Sci. Eur.* **18,** 278-278.

114. Hartwig, A., A. Zeller, T. Schwerdtle, C. Menzel and D. Stueben (2002) Spezies der KFZ-emittierten Platingruppenelemente (PGM) und ihre toxische Wirkung.

115. Deng, J., H. Li, M. Yang and F. Wu (2020) Palladium porphyrin complexes for photodynamic cancer therapy: effect of porphyrin units and metal. *Photochem. Photobiol. Sci.* .

116. Koudinova, N. V., J. H. Pinthus, A. Brandis, O. Brenner, P. Bendel, J. Ramon, Z. Eshhar, A. Scherz and Y. Salomon (2003) Photodynamic therapy with Pd-bacteriopheophorbide (TOOKAD): Successful in vivo treatment of human prostatic small cell carcinoma xenografts. *Int. J. Cancer* **104,** 782-789.

117. Wei, J., J. Li, D. Sun, Q. Li, J. Ma, X. Chen, X. Zhu and N. Zheng (2018) A novel theranostic nanoplatform based on Pd@ Pt-PEG-Ce6 for enhanced photodynamic therapy by modulating tumor hypoxia microenvironment. *Adv. Funct. Mater.* **28,** 1706310.

118. Mfouo-Tynga, I., A. El-Hussein, M. AbdelHarith and H. Abrahamse (2014) Photodynamic ability of silver nanoparticles in inducing cytotoxic effects in breast and lung cancer cell lines. *Int. J. Nanomed.* **9,** 3771-3780.

119. El-Hussein, A. (2016) Study DNA damage after photodynamic therapy using silver nanoparticles with A549 cell line. *J. Nanomed. Nanotechnol.* **7,** 1000346.

120. Shivashankarappa, A. and K. R. Sanjay (2019) Photodynamic therapy on skin melanoma and epidermoid carcinoma cells using conjugated 5-aminolevulinic acid with microbial synthesised silver nanoparticles. *J. Drug Target.* **27,** 434-441.

121. Erdogan, O., M. Abbak, G. M. Demirbolat, F. Birtekocak, M. Aksel, S. Pasa and O. Cevik (2019) Green synthesis of silver nanoparticles via Cynara scolymus leaf extracts: The characterization, anticancer potential with photodynamic therapy in MCF7 cells. *PLOS ONE* **14,** e0216496.

122. Yu, Y., J. Geng, E. Y. X. Ong, V. Chellappan and Y. N. Tan (2016) Bovine Serum Albulmin Protein-Templated Silver Nanocluster (BSA-Ag13): An Effective Singlet Oxygen Generator for Photodynamic Cancer Therapy. *Adv. Healthc. Mater.* **5,** 2528-2535.

123. Silva, A. R. d., A. C. Pelegrino, A. C. Tedesco and R. A. Jorge (2008) Photodynamic activity of chloro (5, 10, 15, 20-tetraphenylporphyrinato) indium (III). *J. Braz. Chem. Soc.* **19,** 491-501.

124. da Silva, A. R., N. M. Inada, D. Rettori, M. O. Baratti, A. E. Vercesi and R. A. Jorge (2009) In vitro photodynamic activity of chloro(5,10,15,20-tetraphenylporphyrinato)indium(III) loaded-poly(lactide-co-glycolide) nanoparticles in LNCaP prostate tumour cells. *J. Photochem. Photobiol.* **94,** 101-112.

125. Selman, S. H., D. ALBRECHT, R. W. KECK, P. BRENNAN and S. KONDO (2001) Studies of tin ethyl etiopurpurin photodynamic therapy of the canine prostate. *J. Urol.* **165,** 1795-1801.

126. Seidl, C., J. Ungelenk, E. Zittel, T. Bergfeldt, J. P. Sleeman, U. Schepers and C. Feldmann (2016) Tin tungstate nanoparticles: a photosensitizer for photodynamic tumor therapy. *ACS nano* **10,** 3149-3157.

127. Feng, L., R. Zhao, B. Liu, F. He, S. Gai, Y. Chen and P. Yang (2020) Near-Infrared Upconversion Mesoporous Tin Oxide Bio-Photocatalyst for H2O2-Activatable O2-Generating Magnetic Targeting Synergetic Treatment. *ACS Appl. Mater. Interfaces* **12,** 41047-41061.

128. Vaupel, P., K. Schlenger, C. Knoop and M. Höckel (1991) Oxygenation of human tumors: evaluation of tissue oxygen distribution in breast cancers by computerized O2 tension measurements. *Cancer Res.* **51,** 3316-3322.

129. Brahimi-Horn, M. C., J. Chiche and J. Pouysségur (2007) Hypoxia and cancer. *J. Mol. Med.* **85,** 1301-1307.

130. Maggiorella, L., G. Barouch, C. Devaux, A. Pottier, E. Deutsch, J. Bourhis, E. Borghi and L. Levy (2012) Nanoscale radiotherapy with hafnium oxide nanoparticles. *Future Oncol.* **8,** 1167-1181.

131. Mendoza, J. G., M. A. Frutis, G. A. Flores, M. G. Hipólito, A. M. Cerda, J. A. Nieto, T. R. Montalvo and C. Falcony (2010) Synthesis and characterization of hafnium oxide films for thermo and photoluminescence applications. *Appl. Radiat. Isot.* **68,** 696-699.

132. Chen, M.-H., N. Hanagata, T. Ikoma, J.-Y. Huang, K.-Y. Li, C.-P. Lin and F.-H. Lin (2016) Hafnium-doped hydroxyapatite nanoparticles with ionizing radiation for lung cancer treatment. *Acta Biomater.* **37,** 165-173.

133. Zuo, H., J. Tao, H. Shi, J. He, Z. Zhou and C. Zhang (2018) Platelet-mimicking nanoparticles co-loaded with W18O49 and metformin alleviate tumor hypoxia for enhanced photodynamic therapy and photothermal therapy. *Acta Biomater.* **80,** 296-307.

134. Kalluru, P., R. Vankayala, C. S. Chiang and K. C. Hwang (2013) Photosensitization of singlet oxygen and in vivo photodynamic therapeutic effects mediated by PEGylated W18O49 nanowires. *Angew. Chem.* **125,** 12558-12562.

135. Sheng, J., L. Zhang, L. Deng, Y. Han, L. Wang, H. He and Y.-N. Liu (2020) Fabrication of dopamine enveloped WO3− x quantum dots as single-NIR laser activated photonic nanodrug for synergistic photothermal/photodynamic therapy against cancer. *Chem. Eng. J.* **383,** 123071.

136. Wang, S. B., C. Zhang, X. H. Liu, Z. X. Chen, S. Y. Peng, Z. L. Zhong and X. Z. Zhang (2019) A Tungsten Nitride-Based O2 Self-Sufficient Nanoplatform for Enhanced Photodynamic Therapy against Hypoxic Tumors. *Adv.Ther.* **2,** 1900012.

137. Borisov, S. M., R. F. Einrem, A. B. Alemayehu and A. Ghosh (2019) Ambient-temperature near-IR phosphorescence and potential applications of rhenium-oxo corroles. *Photochem. Photobiol. Sci.* **18,** 1166-1170.

138. Einrem, R. F., A. B. Alemayehu, S. M. Borisov, A. Ghosh and O. A. Gederaas (2020) Amphiphilic Rhenium-Oxo Corroles as a New Class of Sensitizers for Photodynamic Therapy. *ACS Omega* **5,** 10596-10601.

139. Pan, Z.-Y., D.-H. Cai and L. He (2020) Dinuclear phosphorescent rhenium (I) complexes as potential anticancer and photodynamic therapy agents. *Dalton Trans.* **49,** 11583-11590.

140. Milkevitch, M., H. Storrie, E. Brauns, K. J. Brewer and B. W. Shirley (1997) A new class of supramolecular, mixed-metal DNA-binding agents: The interaction of RuII, PtII and OsII, PtII bimetallic complexes with DNA. *Inorg. Chem.* **36,** 4534-4538.

141. Roque, J. A., P. C. Barrett, H. D. Cole, L. M. Lifshits, G. Shi, S. Monro, D. von Dohlen, S. Kim, N. Russo and G. Deep (2020) Breaking the barrier: an osmium photosensitizer with unprecedented hypoxic phototoxicity for real world photodynamic therapy. *Chem. Sci.* **11,** 9784-9806.

142. Lazic, S., P. Kaspler, G. Shi, S. Monro, T. Sainuddin, S. Forward, K. Kasimova, R. Hennigar, A. Mandel and S. McFarland (2017) Novel Osmium-based Coordination Complexes as Photosensitizers for Panchromatic Photodynamic Therapy. *Photochem. Photobiol.* **93,** 1248-1258.

143. Mandel, A. (2020) Vaccine containing cancer cells inactivated by photodynamic treatment with metal-based coordination complexes, and immunotherapy method using same. Google Patents.

144. Zhang, P., Y. Wang, K. Qiu, Z. Zhao, R. Hu, C. He, Q. Zhang and H. Chao (2017) A NIR phosphorescent osmium (II) complex as a lysosome tracking reagent and photodynamic therapeutic agent. *Chem. Commun.* **53,** 12341-12344.

145. Yuan, B., J. Liu, R. Guan, C. Jin, L. Ji and H. Chao (2019) Endoplasmic reticulum targeted cyclometalated iridium (iii) complexes as efficient photodynamic therapy photosensitizers. *Dalton Trans.* **48,** 6408-6415.

146. Huang, H., S. Banerjee, K. Qiu, P. Zhang, O. Blacque, T. Malcomson, M. J. Paterson, G. J. Clarkson, M. Staniforth and V. G. Stavros (2019) Targeted photoredox catalysis in cancer cells. *Nat. Chem.* **11,** 1041-1048.

147. Zhao, J., K. Yan, G. Xu, X. Liu, Q. Zhao, C. Xu and S. Gou (2020) An Iridium (III) Complex Bearing a Donor–Acceptor–Donor Type Ligand for NIR-Triggered Dual Phototherapy. *Adv. Funct. Mater.*, 2008325.

148. Boreham, E. M., L. Jones, A. N. Swinburne, M. Blanchard-Desce, V. Hugues, C. Terryn, F. Miomandre, G. Lemercier and L. S. Natrajan (2015) A cyclometallated fluorenyl Ir (III) complex as a potential sensitiser for two-photon excited photodynamic therapy (2PE-PDT). *Dalton Trans.* **44,** 16127-16135.

149. Lange, C. and P. J. Bednarski (2018) Evaluation for synergistic effects by combinations of photodynamic therapy (PDT) with temoporfin (mTHPC) and Pt (II) complexes carboplatin, cisplatin or oxaliplatin in a set of five human cancer cell lines. *Int. J. Mol. Sci.* **19,** 3183.

150. Crul, M., R. Van Waardenburg, J. Beijnen and J. Schellens (2002) DNA-based drug interactions of cisplatin. *Cancer Treat. Rev.* **28,** 291-303.

151. Comella, P., R. Casaretti, C. Sandomenico, A. Avallone and L. Franco (2009) Role of oxaliplatin in the treatment of colorectal cancer. *Ther. Clin. Risk Manag.* **5,** 229.

152. Doherty, R. E., I. V. Sazanovich, L. K. McKenzie, A. S. Stasheuski, R. Coyle, E. Baggaley, S. Bottomley, J. A. Weinstein and H. E. Bryant (2016) Photodynamic killing of cancer cells by a Platinum (II) complex with cyclometallating ligand. *Sci. Rep.* **6,** 1-9.

153. Rizvi, I., J. P. Celli, C. L. Evans, A. O. Abu-Yousif, A. Muzikansky, B. W. Pogue, D. Finkelstein and T. Hasan (2010) Synergistic enhancement of carboplatin efficacy with photodynamic therapy in a three-dimensional model for micrometastatic ovarian cancer. *Cancer Res.* **70,** 9319-9328.

154. Choi, Y., J. E. Chang, S. Jheon, S. J. Han and J. K. Kim (2018) Enhanced production of reactive oxygen species in HeLa cells under concurrent low‐dose carboplatin and Photofrin® photodynamic therapy. *Oncol. Rep.* **40,** 339-345.

155. Cheng, Y., Y. Chang, Y. Feng, N. Liu, X. Sun, Y. Feng, X. Li and H. Zhang (2017) Simulated Sunlight-Mediated Photodynamic Therapy for Melanoma Skin Cancer by Titanium-Dioxide-Nanoparticle–Gold-Nanocluster–Graphene Heterogeneous Nanocomposites. *Small* **13,** 1603935.

156.    Stuchinskaya, T., M. Moreno, M. J. Cook, D. R. Edwards and D. A. Russell (2011) Targeted photodynamic therapy of breast cancer cells using antibody–phthalocyanine–gold nanoparticle conjugates. *Photochem. Photobiol. Sci.* **10,** 822-831.

157.    Calavia, P. G., I. Chambrier, M. J. Cook, A. H. Haines, R. A. Field and D. A. Russell (2018) Targeted photodynamic therapy of breast cancer cells using lactose-phthalocyanine functionalized gold nanoparticles. *J. Colloid Interface Sci.* **512,** 249-259.

158.    Astorgues-Xerri, L., M. E. Riveiro, A. Tijeras-Raballand, M. Serova, C. Neuzillet, S. Albert, E. Raymond and S. Faivre (2014) Unraveling galectin-1 as a novel therapeutic target for cancer. *Cancer Treat. Rev.* **40,** 307-319.

159.    Shrestha, S., J. Wu, B. Sah, A. Vanasse, L. N. Cooper, L. Ma, G. Li, H. Zheng, W. Chen and M. P. Antosh (2019) X-ray induced photodynamic therapy with copper-cysteamine nanoparticles in mice tumors. *Proc. Natl. Acad. Sci.* **116,** 16823-16828.

160.    Sengar, P., P. Juárez, A. Verdugo-Meza, D. L. Arellano, A. Jain, K. Chauhan, G. A. Hirata and P. G. Fournier (2018) Development of a functionalized UV-emitting nanocomposite for the treatment of cancer using indirect photodynamic therapy. *J. Nanobiotechnol.* **16,** 1-19.

161.    Fernández, M., F. Javaid and V. Chudasama (2018) Advances in targeting the folate receptor in the treatment/imaging of cancers. *Chem. Sci.* **9,** 790-810.

162.    Furukawa, K., T. Okunaka, H. Yamamoto, T. Tsuchida, J. Usuda, H. Kumasaka, J. Ishida, C. Konaka and H. Kato (1999) Effectiveness of photodynamic therapy and Nd-YAG laser treatment for obstructed tracheobronchial malignancies. *Diagn. Ther. Endosc.* **5,** 161-166.

163.    Nie, Z., X. Ke, D. Li, Y. Zhao, L. Zhu, R. Qiao and X. L. Zhang (2019) NaYF4: Yb, Er, Nd@ NaYF4: Nd upconversion nanocrystals capped with Mn: TiO2 for 808 nm NIR-triggered photocatalytic applications. *J. Phys. Chem. C* **123,** 22959-22970.

164.    Lu, H., W. Zhang, X. Zhang, J. Rong, P. Gao, T. Liu, B. Lan and W. Liu (2018) Novel nano particle-photosensitizer conjugate for treating deep tumor by X-ray motivated photodynamic therapy, preparation method and its application in cancer therapy. pp. 17pp. Fourth Military Medical University, Peop. Rep. China .

165. Bulin, A.-L., C. Truillet, R. Chouikrat, F. Lux, C. Frochot, D. Amans, G. Ledoux, O. Tillement, P. Perriat and M. Barberi-Heyob (2013) X-ray-induced singlet oxygen activation with nanoscintillator-coupled porphyrins. *J. Phys. Chem.* **117,** 21583-21589.

166. Zhang, Y., G. K. Das, V. Vijayaragavan, Q. C. Xu, P. Padmanabhan, K. K. Bhakoo, S. Tamil Selvan and T. T. Y. Tan (2014) "Smart" theranostic lanthanide nanoprobes with simultaneous up-conversion fluorescence and tunable T1-T2 magnetic resonance imaging contrast and near-infrared activated photodynamic therapy. *Nanoscale* **6,** 12609-12617.

167. Guerra, Á. R., T. F. Aparicio, I. B. Bayonas, A. P. Martínez, V. M. Guillermo, D. J. Peralta, C. C. George, B. Pietricica, E. I. Morejón and A. R. Sánchez (2018) Outpatient Holmium laser fulguration: A safe procedure for treatment of recurrence of nonmuscle invasive bladder cancer. *Actas Urológicas Españolas* **42,** 309-315.

168. Li, C., L. Guo, P. Wang, L. Shi, X. Sun, C. Hu, G. Zhang, L. Zhang, Y. Zhang and X. Wang (2019) ALA-PDT combined with holmium laser therapy of postoperative recurrent extramammary Paget's disease. *Photodiagn. Photodyn. Ther.* **27,** 92-94.

169. Šmucler, R. and M. Vlk (2008) Combination of Er: YAG laser and photodynamic therapy in the treatment of nodular basal cell carcinoma. *Lasers Surg. Med.* **40,** 153-158.

170. Deng, R., B. Zheng and J. Zhou (2019) Method for directly exciting organic molecule triplet state by rare earth ion and application of rare earth ion in photodynamic therapy, photocatalysis and drug release. pp. 19pp. Zhejiang University, Peop. Rep. China .

171. Yusupov, A., S. Goncharov, I. Zalevskii, V. Paramonov and A. Kurkov (2010) Raman fiber laser for the drug-free photodynamic therapy. *Laser Physics.* **20,** 357-359.

172. Ross, H., J. Smelstoys, G. Davis, A. Kapatkin, F. Del Piero, E. Reineke, H. Wang, T. Zhu, T. Busch and A. Yodh (2006) Photodynamic therapy with motexafin lutetium for rectal cancer: a preclinical model in the dog. *J. Surg. Res.* **135,** 323-330.

173. Kulkarni, G. (2017) Intravesical Photodynamic Therapy (PDT) in BCG Refractory High-Risk Non-muscle Invasive Bladder Cancer (NMIBC) Patients. University Health Network, Toronto.

174. Trachtenberg, J., A. Bogaards, R. Weersink, M. Haider, A. Evans, S. McCluskey, A. Scherz, M. Gertner, C. Yue and S. Appu (2007) Vascular targeted photodynamic therapy with palladium-bacteriopheophorbide photosensitizer for recurrent prostate cancer following

definitive radiation therapy: assessment of safety and treatment response. *J. Urol.* **178,** 1974-1979.

175. Mang, T. S., R. Allison, G. Hewson, W. Snider and R. Moskowitz (1998) A phase II/III clinical study of tin ethyl etiopurpurin (Purlytin)-induced photodynamic therapy for the treatment of recurrent cutaneous metastatic breast cancer. *Cancer J.* **4,** 378-384.

176. Du, K., R. Mick, T. Busch, T. Zhu, J. Finlay, G. Yu, A. Yodh, S. Malkowicz, D. Smith and R. Whittington (2006) Preliminary results of interstitial motexafin lutetium-mediated PDT for prostate cancer. *Lasers Med. Sci.* **38,** 427-434.

177. Patel, H., R. Mick, J. Finlay, T. C. Zhu, E. Rickter, K. A. Cengel, S. B. Malkowicz, S. M. Hahn and T. M. Busch (2008) Motexafin lutetium-photodynamic therapy of prostate cancer: short-and long-term effects on prostate-specific antigen. *Clin. Cancer Res.* **14,** 4869-4876.

178. Verigos, K., D. C. H. Stripp, R. Mick, T. C. Zhu, R. Whittington, D. Smith, A. Dimofte, J. Finlay, T. M. Busch and Z. A. Tochner (2006) Updated results of a phase I trial of motexafin lutetium-mediated interstitial photodynamic therapy in patients with locally recurrent prostate cancer. *J. Environ. Pathol. Toxicol. Oncol.* **25**.

179. Hahn, S. M. (2003) Photodynamic Therapy With Lutetium Texaphyrin in Treating Patients With Locally Recurrent Prostate Cancer. University of Pennsylvania, Pennsylvania.

180. Comerci, J. (2003) Photodynamic Therapy Using Lutetium Texaphyrin in Treating Patients With Cervical Intraepithelial Neoplasia. University of Pittsburgh, Pennsylvania.

181. Dimofte, A., T. C. Zhu, S. M. Hahn and R. A. Lustig (2002) In vivo light dosimetry for motexafin lutetium-mediated PDT of recurrent breast cancer. *Lasers Med. Sci.* **31,** 305-312.

182. Coleman, J. (2020) ENdoluminal LIGHT ActivatED Treatment of Upper Tract Urothelial Cancer (ENLIGHTED) Study Memorial Sloan Kettering New York.

## FIGURE CAPTIONS

**Figure 1**. Structure of aluminium phthalocyanine chloride (AlClPc).

**Figure 2.** Structures of the oxidovanadium(IV) complexes, [VO(salmet)(N-N)], [VO(saltrp)(N-N)], [VO($L^2$)Cl$_2$], [VO(cat)(L)], and [VO(dopa-NBD)(L)], respectively.

**Figure 3**. Structures of [Fe(L)(tpy-BODIPY)] and metallocorrole, Fe-2c , respectively.

**Figure 4.** Structures of the cobalt(III) complexes.

**Figure 5**. Structures of the cobalt(II) complexes, [Co(ph-tpy)$_2$]$^{2+}$, [Co(an-tpy)$_2$] $^{2+}$, and [Co(py-tpy)$_2$] $^{2+}$, respectively.

**Figure 6.** Normal fibroblast and melanoma cells after 5 μM and 10 μM administration of Ni(II) ruthenated porphyrin followed by 60 min irradiation with tungsten lamp. Reproduced from Ref. 73 with permission from The Royal Society of Chemistry.

**Figure 7.** Structures of the copper complexes.

**Figure 8**. Structures of the zinc porphyrins (P1-P3).

**Figure 9.** The structures of H$_2$Pp and ZnPp porphyrins.

**Figure 10.** Structure of the ruthenium(II) complex.

**Figure 11.** Structure of Ru-tmxf.

**Figure 12.** Structures of complexes 2 and 3.

**Figure 13**. Structure of complex 4.

**Figure 14.** Structure of complexes 5.

**Figure 15**. Structures of complexes 6 and 7.

**Figure 16.** Schematic representation of the PDT and PTT mechanism of the Ru@SWCNTs anti-cancer properties *in vivo*. Reprinted with permission from Ref. 102. Copyright (2015) American Chemical Society.

**Figure 17.** Structure of Pt(II) 2,6-dipyrido-4-methyl-benzenechloride.

**Figure 18.** Structure of Temoporofin.

**Table 1.** Advancements of transition metal complexes and PDT tested in clinical trials.

| Complexes | Trial phase | Status | Outcomes | Ref. |
|---|---|---|---|---|
|  | Phase Ib | Completed | TDL1433 safety and tolerability in non-muscle invasive bladder cancer patients was successfully established. | (173) |
|  | Phase III | Recruiting | Tookad treating patients with upper tract urothelial cancer with Tookad and PDT. | (182) |
| | Phase I/IIa | Terminated | No viable prostate tumors were found 7 days post treatment; however, MRI results were considered inconclusive. | (174) |
|  | Phase III | Completed | All patients responded to Purlytin treatment of recurrent breast cancer with a decrease in tumor volume. | (175) |
| Complexes | Trial phase | Status | Outcomes | Ref. |

| | Phase I | Terminated | Motexafin lutetium safely treating of recurrent prostate adenocarcinoma. | (179) |
|---|---|---|---|---|
| | Phase II | Terminated | Measured the irradiance and fluence rate on the tissue surface or patients with recurrent breast cancer. | (181) |
| | | | | |

php_13467_f1.jpg

php_13467_f2.jpg

[Fe(L)(tpy-BODIPY)]           Fe-**2b**

php_13467_f3.jpg

php_13467_f4.jpg

[Co(ph-tpy)₂]²⁺          [Co(an-tpy)₂]²⁺          [Co(py-tpy)₂]²⁺

php_13467_f5.jpg

php_13467_f6.jpg

php_13467_f7.jpg

php_13467_f8.jpg

php_13467_f9.jpg

H₂Pp
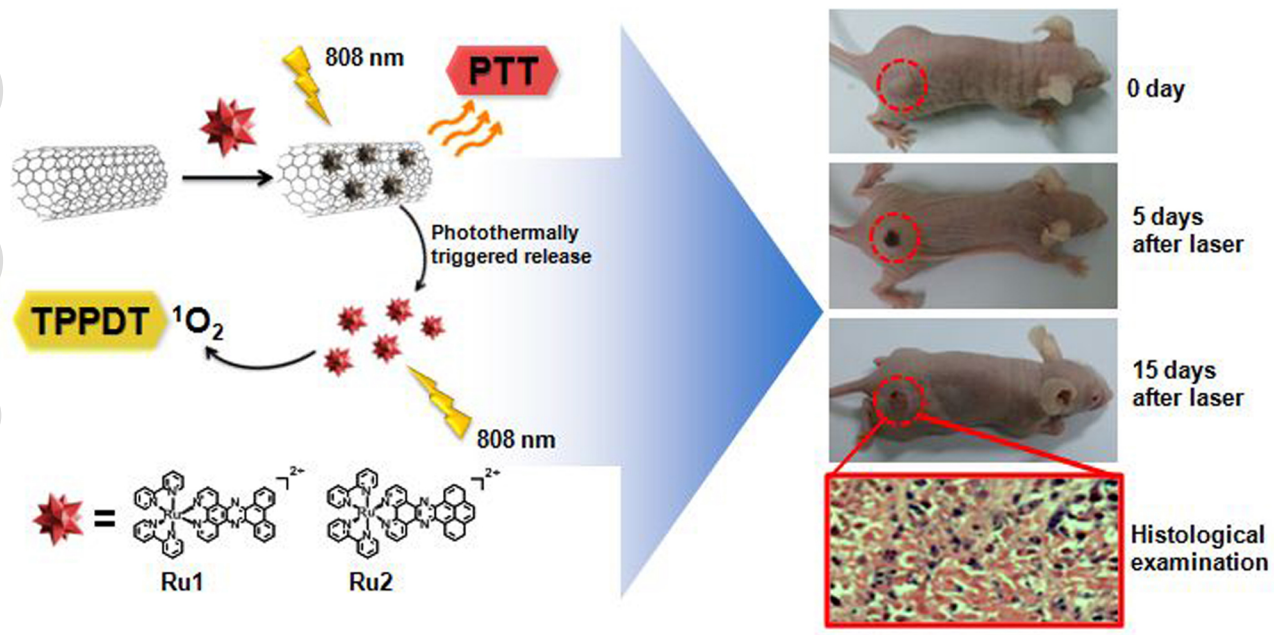
ZnPp

php_13467_f10.jpg
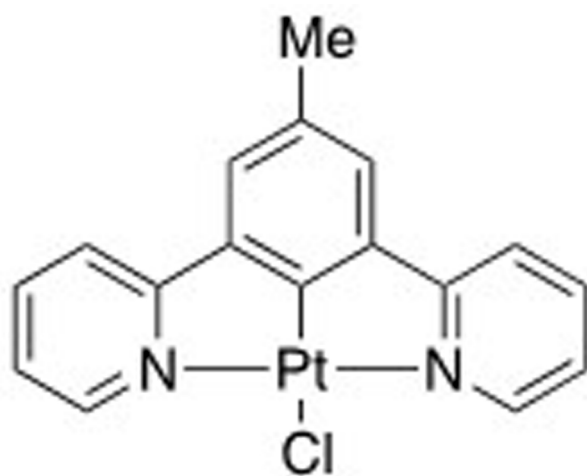
php_13467_f11.jpg
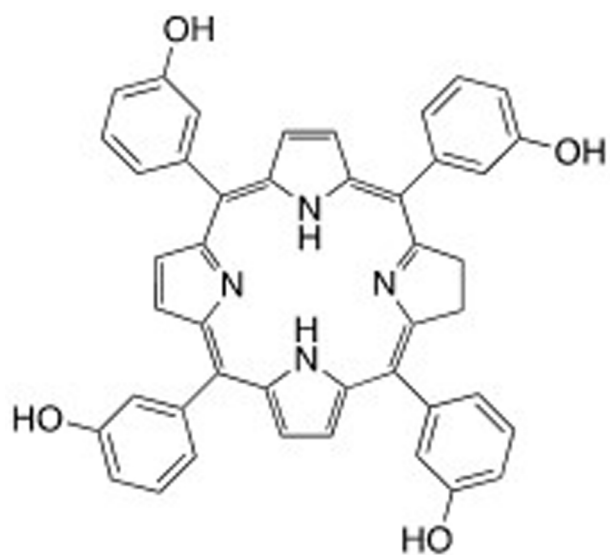
php_13467_f12.jpg

php_13467_f13.jpg
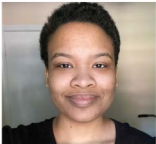
php_13467_f14.jpg

php_13467_f15.jpg

php_13467_f16.jpg
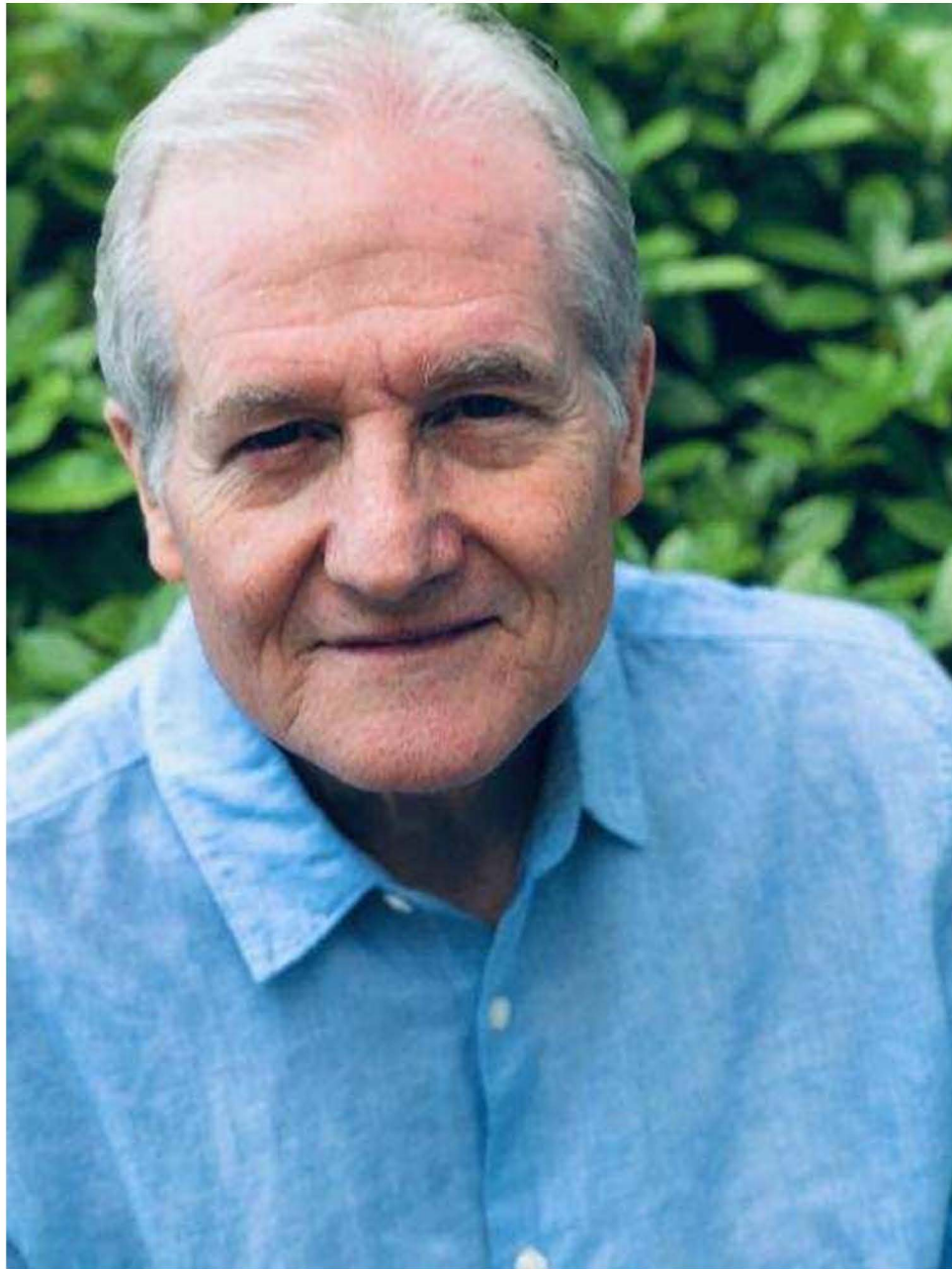
php_13467_f17.jpg

php_13467_f18.jpg

Chloe Smith is an undergraduate biology major and a Maximizing Access to Research Careers (MARC) Scholar at Old Dominion University (ODU). She works with Dr. Alvin Holder and his collaborator, Dr. Stephen Beebe on researching anti-cancer activities of transition metal complexes. She has worked in Dr. Riyaz Basha's laboratory at the University of North Texas Health Science Centre on testing transition metal complexes on pediatric cancer. In Dr. Basha's laboratory, she was a co-author on a pancreatic cancer review and a colon cancer textbook chapter. Her research interests include evolution of diseases and treating cancer using novel chemotherapies and immunotherapies.

Lindsay Days is a biochemistry major at Old Dominion University. She is a junior and a MARC Scholar at ODU She was a recipient of the John and Kate Broderick Opportunity Scholarship and was a recipient of the Perry Honor College Research Grant for her research in synthesizing anti-cancer drugs for the treatment of triple negative breast cancer. Her research interests include anti-cancer, genomic, and biomedical research. She hopes to pursue a Ph.D. degree in the biomedical sciences.

Duaa Alajroush is a second year Ph.D. student. She is working in the laboratory of Dr. Alvin Holder researching the effect of transition-metal complexes in fighting cancer. She received her B.Sc. degree from King Saud University and her M.S. degree from King Abdulaziz University in Saudi Arabia. Her degree was in Biochemistry. She published her research entitled "*Anti-cancer Activity of Bis (4-bromobenzaldehyde-4-iminacetophenone) Diaquozinc(II) Nitrate Complex against Ehrlich Ascites Carcinoma Cells Induced in Mice*". Her research interests include *in vitro* and *in vivo* studies for cancer therapy.

Khadija Faye is a second-year chemistry Ph.D. student who is working under Dr. Alvin A. Holder's mentorship. She received her bachelor's degree in Biochemistry at ODU, during which she started working

on the synthesis and characterization of several transition metal-based complexes. Her current work and research interests include the synthesis and characterization of metal-based complexes as well as *in vitro* and *in vivo* studies against cancer, specifically triple negative breast cancer.

Yara Khodour is a first year Ph.D. student who rotated in the laboratory of Dr. Alvin Holder. She received her B.S. degree from Birzeit University in Palestine. Her degree was major biology/minor biochemistry. During her undergraduate studies she worked with Dr. Johnny Stiban and published a book chapter with him on iron-sulfur clusters in nucleic acid metabolism. After graduation she worked as a visiting fellow in Prof. Anthony H. Futerman's laboratory at the Weizmann Institute of Science in Israel, while working on ceramide synthases enzymes. Her research interests are sphingolipid biochemistry, cancer therapy, and enzymology.

Prof. Stephen J. Beebe is a Research Professor and one of the founding members of the Frank Reidy Research Center for Bioelectrics at ODU. He received his Ph.D. degree in Medical Sciences (Pharmacology) at the Toledo University College of Medicine (1982); was a postdoctoral fellow in the HHMI, Vanderbilt, and Fulbright and Marshall Scholar, Oslo. He serves/has served on 10 journal editorial boards, published 136 peer-reviewed manuscripts, book chapters, and editorials, trained over 30 students and postdoctoral fellows, and was included in the top 2% of most cited scientist worldwide, 2020. He serves as the Chair of the ODU IACUC.

Prof. Alvin A. Holder is a Professor of Chemistry at ODU. His research focuses bioinorganic and inorganic chemistry and reaction mechanisms. The primary theme for his research is solving world problems, including cancer and the dwindling fossil fuels reserves, with inorganic elements. Dr. Holder earned a B.Sc.

degree in special chemistry and a Ph.D. degree in inorganic chemistry from The University of the West Indies (UWI), Mona Campus, Jamaica.